Supplementary information

Ethynylene-linked multifunctional benzoxazines: effect of ethynylene group and packing on thermal behavior

Masanobu Muraoka,[†] Masahide Goto,[†] Masaki Minami,[‡] Dayang Zhou,[§] Takeyuki Suzuki,[§] Tatsuo Yajima,[†] Jun'ichi Hayashi,[⊥] Hiromitsu Sogawa,[†] Fumio Sanda*[,†]

[†] Department of Chemistry and Materials Engineering, Faculty of Chemistry, Materials and Bioengineering, Kansai University, 3-3-35 Yamate-cho, Suita, Osaka 564-8680, Japan

[‡] Chemicals R&D Group, HPM Research and Development Department, High Performance Materials Company, ENEOS Corporation, 8 Chidori-cho, Naka-ku, Yokohama, Kanagawa 231-0815, Japan

[§] Comprehensive Analysis Center, SANKEN, Osaka University, Ibaraki, Osaka 567-0047, Japan

[⊥] Department of Chemical, Energy and Environmental Engineering, Faculty of Environmental and Urban Engineering, Kansai University, 3-3-35 Yamate-cho, Suita, Osaka 564-8680, Japan

* Corresponding Author

Experimental section

Measurements. Solution state ^{1}H and ^{13}C NMR spectra were recorded on JEOL JNM-ECZ400, JNM-ECS400 and BRUKER AVANCEⅢ700 spectrometers. Solid state ^{13}C NMR spectra were recorded on a BRUKER AVANCEⅢ600WB. Melting points (mp) were measured on a Yanaco micro melting point apparatus. IR absorption spectra were measured on a JASCO FT/IR-4100 spectrophotometer. ESI-TOF mass spectra were measured on an Applied Biosystems APCI-3000 and a Shimadzu LCMS-IT-TOF. Single crystal X-ray analysis was performed using a Rigaku RAXIS imaging plate area detector with graphite-monochromated Mo-Kα radiation (λ = 0.71075 Å). A crystal was mounted on a nylon loop at 123 K. The structure was solved and refined using the Olex2[S1] and SHELX[S2,S3] programs. XRD spectra were measured on a BRUKER D2 PHASER with Cu-Kα radiation. The ring-opening crosslinking reaction of the samples was carried out in a Nitto small electric furnace mini-BSI. DSC was measured on a Rigaku Thermoplus EVO DSC 8230 under air. TGA was measured with a Shimadzu thermogravimetric analyzer TGA-50 with a heating rate of 10 °C min^{-1} from 50 °C to 800 °C under nitrogen at a flow rate of 50 mL min^{-1}. Densities were measured with a Shimadzu gas pycnometer AccuPyc II 1340 at 26 °C, in which averages of 10 measurements were employed. BET specific surface area and micropore volume were measured by using N_2 adsorption isotherm at 77 K on a Microtrac BEL, BELSORP-mini II. CO_2 adsorption isotherms were measured at 298 K on a Microtrac BEL, BELSORP-28. Field emission scanning electron microscopy (FE-SEM) observation was performed on a JEOL JSM 6700f.

Reagents. Pd-Bz was obtained from Seika Corporation. The other reagents were purchased and used without purification unless otherwise stated. *p*-Ethynylaniline (FUJIFILM Wako Pure Chemical Corporation), salicylaldehyde (Tokyo Chemical Industry Co., TCI), ethanol (EtOH, FUJIFILM Wako), sodium borohydride ($NaBH_4$, TCI), paraformaldehyde (FUJIFILM Wako), 1,4-dioxane (FUJIFILM Wako), iodobenzene (FUJIFILM Wako), triphenylphosphine (FUJIFILM Wako), copper(I) iodide (CuI(I), NACALAI TESQUE, INC.), bis(triphenylphosphine)palladium(II)dichloride, tetrahydrofuran (THF) with stabilizer (FUJIFILM Wako), 2-dicyclohexylphosphino-2',4',6'-triisopropyl-1,1'-biphenyl (XPhos, TCI), triethylamine (Et_3N, NACALAI), 1,4-diiodobenzene (TCI), 1,3,5-tribromobenzene (TCI), potassium iodide (KI, NACALAI), 1,3-dimethyl-2-imidazolidinone (DMI, FUJIFILM Wako), anhydrous magnesium sulfate ($MgSO_4$, FUJIFILM Wako), hexane (NACALAI), dichloromethane (CH_2Cl_2, NACALAI), sodium hydroxide (NaOH, NACALAI) were used without purification. Solvents used in the reaction under Ar and N_2 were dehydrated over molecular sieves 4A1/16 and degassed by Ar and N_2 gas bubbling, respectively.

Synthesis of 3-(4-Ethynyl)phenyl-3,4-dihydro-1,3-benzoxazine (6)

Compound **6** was synthesized according to Scheme S1. The synthetic procedures follow the scheme.

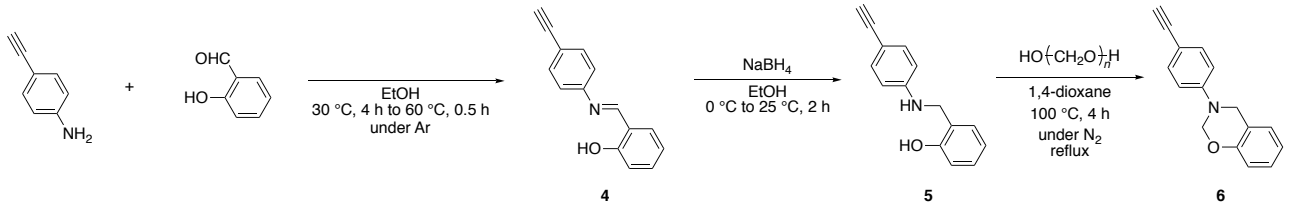

Scheme S1 Synthesis of **6**.

(*E*)-2-(((4-ethynylphenyl)imino)methyl)phenol (4)

p-Ethynylaniline (10.6 g, 90.3 mmol) was fed in a glass flask. It was degassed and filled with Ar. EtOH (180 mL) was added to the flask, and the resulting solution was stirred at room temperature for 5 min. It was heated to 30 °C; then salicylaldehyde (9.60 mL, 90.3 mmol) was added to the solution. The resulting mixture was stirred at 30 °C for 4 h, and then stirred at 60 °C for 0.5 h. The mixture was cooled with ice water to precipitate a solid mass. It was separated by filtration using a Kiriyama funnel, and dried under reduced pressure overnight to obtain yellow solid **4** (14.4 g, 64.9 mmol). Yield 72%. ^{1}H NMR (400 MHz, $CDCl_3$): δ 3.12 (s, 1H, CH≡C), 6.92–7.03 (m, 1H, Ar), 7.01–7.03 (m, 1H, Ar), 7.15–7.28 (m, 3H, Ar), 7.33–7.44 (m, 2H, Ar), 7.51–7.59 (m, 2H, Ar), 8.60 (s, 1H, N=CH) ppm.

2-(((4-Ethynylphenyl)amino)methyl)phenol (5)

Compound **4** (14.4 g, 64.9 mmol) was fed in a glass flask, EtOH (300 mL) was added to the flask, and the resulting solution was cooled to 0 °C and stirred for 5 min. $NaBH_4$ (1.84 g, 64.9 mmol) was added to the solution, and the resulting mixture was stirred at room temperature for 2 h. Pure water (10 mL) was added to the mixture, and the resulting mixture was stirred for a while to dissolve residual

$NaBH_4$. Then the reaction mixture was sequentially washed with CH_2Cl_2 (300 mL), 1 M NaOH aq (100 mL × 3). Solvents were evaporated under reduced pressure overnight to obtain brownish white solid **5** (13.3 g, 59.4 mmol). Yield 92%. ^{1}H NMR (400 MHz, $CDCl_3$): δ 2.98 (s, 1H, CH≡C), 4.10 (s, 1H, –NH–), 4.40 (s, 2H, N–CH_2–), 6.66–6.78 (m, 2H, Ar), 6.87–6.97 (m, 2H, Ar), 7.16–7.27 (m, 2H, Ar), 7.34–7.38 (m, 2H, Ar), 7.46 (s, 1H, –OH) ppm.

3-(4-Ethynylphenyl)-3,4-dihydro-2*H*-[1,3]benzoxazine (6)[S4]

Compound **5** (13.3 g, 59.4 mmol) and paraformaldehyde (2.05 g, 67.4 mmol) were fed in a glass flask. It was degassed and filled with N_2. 1,4-Dioxane (200 mL) was added to the flask, and the resulting mixture was stirred at 100 °C for 4 h. The mixture was cooled to room temperature, and CH_2Cl_2 (90 mL) was added to the mixture. The resulting solution was washed with 1 M NaOH aq (30 mL × 3) to obtain a clear yellow solution. The organic phase was separated, and the solvents were evaporated under reduced pressure to obtain yellow solid **6** (13.4 g, 57.0 mmol). Yield 96%. ^{1}H NMR (400 MHz, $CDCl_3$): δ 2.98 (s, 1H, CH≡C), 4.63 (s, 2H, Ar–CH_2–N), 5.35 (s, 2H, O–CH_2–N), 6.80–6.93 (m, 2H, Ar), 6.98–7.17 (m, 4H, Ar), 7.37–7.45 (m, 2H, Ar) ppm.

1,3,5-Triiodobenzene[S5,S6]

The title compound was synthesized according to Scheme S2. The synthetic procedure follows the scheme.

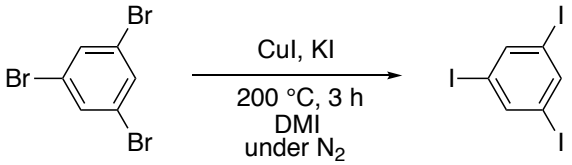

Scheme S2 Synthesis of 1,3,5-triiodobenzene.

1,3,5-Tribromobenzene (4.00 g), CuI (5.78 g), KI (6.71 g) were fed in a glass flask. It was degassed and filled with N_2. DMI (70 mL) was added to the flask, and the resulting mixture was stirred at 200°C for 2 h. The reaction mixture was cooled with ice water to precipitate a solid mass. It was separated by filtration and washed with diethyl ether/brine to obtain 1,3,5-tribromobenzene as white solid (2.45 g). Yield 42%. ^{1}H NMR (400 MHz, $CDCl_3$): δ 7.19 (s, 3H) ppm.

3-(4-(Phenylethynyl)phenyl)-3,4-dihydro-2*H*-[1,3]benzoxazine (1)

The title compound was synthesized according to Scheme 1. The synthetic procedure is as follows. Compound **6** (4.24 g, 17.9 mmol), PPh_3 (0.967 g, 3.59 mmol), CuI (6.99×10^{-2} g, 0.359 mmol) and $(PPh_3)_2PdCl_2$ (0.132 g, 0.179 mmol) were fed in a glass flask. It was degassed and filled with Ar. THF (30 mL), Et_3N (25 mL) and iodobenzene (2.0 mL, 17.9 mmol) were added to the flask, and the resulting mixture was stirred at 80 °C for 24 h under light shielding. Then the reaction mixture was sequentially washed with CH_2Cl_2 (90 mL), 1 M NaOH aq (30 mL × 3), and pure water (30 mL). The organic phase was separated, and solvents were evaporated under reduced pressure overnight. a yellow solid was obtained, which was purified by recrystallization with CH_2Cl_2/hexane to give a yellowish-white solid **1** (4.10 g, 13.2 mmol). Yield 73%, mp = 134–137 °C. IR (KBr disk): 3279, 3042, 2858, 2818, 2212, 1884, 1609, 1523, 1259, 1008, 816, 751, 690, 544 cm^{-1}. ^{1}H NMR (400 MHz, DMSO-

d_6): δ 4.71 (s, 2H, Ar–CH_2–N), 5.49 (s, 2H, O–CH_2–N), 6.70–6.73 (m, 1H, Ar), 6.83–6.87 (m, 1H, Ar), 7.04–7.15 (m, 4H, Ar), 7.31–7.40 (m, 5H, Ar), 7.43–7.49 (m, 2H, Ar) ppm. ^{13}C NMR (100 MHz, DMSO-d_6): δ 48.9, 78.3, 88.5, 90.3, 113.8, 116.9, 117.2, 121.2, 121.8, 123.3, 127.8, 128.3, 128.8, 129.2, 131.6, 133.0, 148.4, 154.4 ppm. ESI-MS (*m*/*z*): calcd. 312.1383 ($[C_{22}H_{17}NO + H]^+$), found 312.1362.

1,4-Bis((4-(2*H*-3(4*H*)-[1,3]benzoxazinyl)phenyl)ethynyl)benzene (2)

Compound **2** was synthesized from **6** and 1,4-diiodobenzene in a manner similar to **1**. XPhos was used instead of PPh_3. Yield 70%, yellowish-white solid, mp = 254–258 °C. IR (KBr disk): 3435, 3043, 2918, 2882, 2850, 2213, 1893, 1605, 1522, 1256, 1048, 817, 748, 532 cm^{-1}. ^{1}H NMR (400 MHz, $CDCl_3$): *δ* 4.65 (s, 4H, Ar–CH_2–N), 5.36 (s, 4H, O–CH_2–N), 6.80–6.91 (m, 4H, Ar), 6.99–7.14 (m, 8H, Ar), 7.40–7.43 (m, 8H, Ar) ppm. ^{13}C NMR (175 MHz, $CDCl_3$): *δ* 50.1, 78.6, 88.2, 91.3, 115.2, 117.1, 117.3, 120.7, 121.1, 123.0, 126.8, 128.0, 131.3, 132.8, 148.2, 154.2 ppm. ESI-MS (*m*/*z*): calcd. 545.2224 ($[C_{38}H_{28}N_2O_2 + H]^+$), found 545.2212.

1,3,5-Tris((4-(2*H*-3(4*H*)-[1,3]benzoxazinyl)phenyl)ethynyl)benzene (3)

Compound **3** was synthesized from **6** and 1,3,5-triiodobenzene in a manner similar to **1**. It was purified by recrystallization with CH_2Cl_2/hexane. Yield 64%, yellow solid, mp = 136–140 °C. IR (KBr disk): 3398, 3040, 2893, 2851, 2567, 2360, 2203, 1894, 1782, 1607, 1577, 1512, 1226, 947, 754, 540 cm^{-1}. ^{1}H NMR (400 MHz, DMSO-d_6): *δ* 4.66 (s, 6H, Ar–CH_2–N), 5.44 (s, 6H, O–CH_2–N), 6.65–6.77 (m, 3H, Ar), 6.83–6.91 (m, 3H, Ar), 7.04–7.21 (m, 12H, Ar), 7.33–7.82 (m, 9H, Ar) ppm. ^{13}C NMR (100

MHz, $CDCl_3$): δ 50.1, 78.6, 87.1, 90.6, 115.1, 117.2, 117.3, 120.7, 121.1, 124.3, 126.8, 128.1, 133.0, 133.5, 148.4, 154.4 ppm. ESI-MS (*m*/*z*): calcd. 778.3064 ($[C_{54}H_{39}N_3O_3 + H]^+$), found 778.3049.

Polymerization: typical procedure.

A powdery sample of **1** was fed into an aluminum sample pan. It was placed on a glass petri dish, and heated in a Nitto small electric furnace mini-BSI at 150–300 °C for 2 h under N_2 to obtain Poly(**1**).

Curing Kinetics.

The activation energies (E_a) for curing of **1**–**3** were determined by Ozawa–Flynn–Wall method,[S7–S9] based on the DSC measurements at heating rates of 5, 10, 15, and 20 °C/min (Fig. S38–S40). The values of E_a were calculated using the following equation,

$$\ln(\beta) = -1.052E_a/RT_p + C$$

where β is the heating rate, T_p is the temperature at the exothermic peak maximum, R is the gas constant, and C is a constant. E_a can be obtained from the slope of the plot of $\ln(\beta)$ versus $1/T_p$. The E_a values for curing of **1**, **2** and **3** were 83.52, 133.75 and 67.14 kJ/mol, respectively. It is considered that molecules of **2** are densly packed compared with **1** and **3**, leading to low mobility, resulting in the high E_a.

Computations. DFT calculations were performed with Gaussian 16,[S10] ES64L-G16 Rev C.01, using ωB97X-D functional in conjunction with 6-31G* basis set, running on the supercomputer system, Academic Center for Computing and Media Studies, Kyoto University. Noncovalent interaction plot was performed using NCIPLOT.[S11,S12] MD simulations were performed with LAMMPS 2020,[S13] running on the supercomputer system, Fugaku provided by the RIKEN Center for Computational Science.

CO_2 adsorption. Unlike the corresponding benzoxazine monomers, polybenzoxazines poly(**1**)–poly(**3**) showed no sharp XRD peaks (Fig. S47). It is considered that poly(**1**)–poly(**3**) do not exhibit the regulated angstrom-order molecular alignment observed in the corresponding monomers, while the polymers formed micron/submicron pores that efficiently adsorb CO_2. Physisorption is an effective capture method because of the low energy consumption, high efficiency, easy regeneration and high cost-effectiveness.[S14,S15]

Morphology. The samples of benzoxazines **1**, **2**, **3** and Pd-Bz were observed by FE-SEM after curing to obtain information on the surface morphology (Fig. S52).

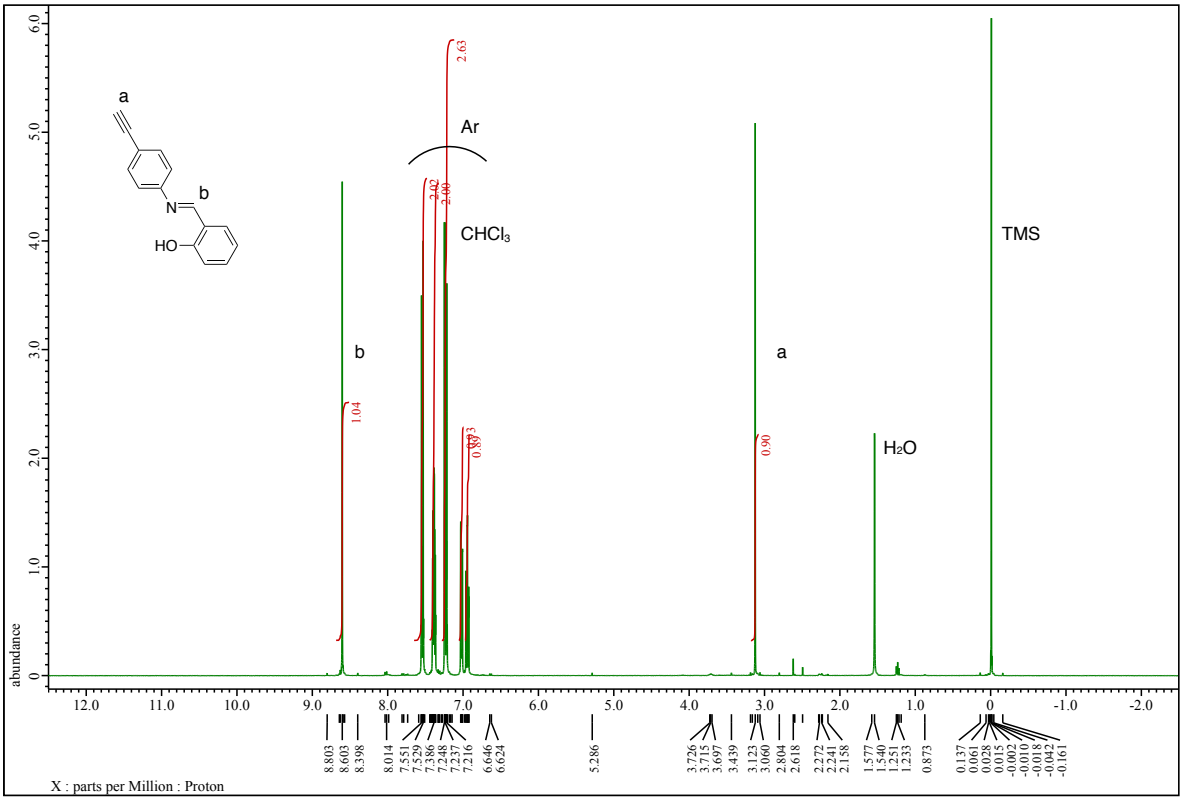

Fig. S1 ^{1}H NMR spectrum of **1** measured at 400 MHz in $CDCl_3$ at 25 °C.

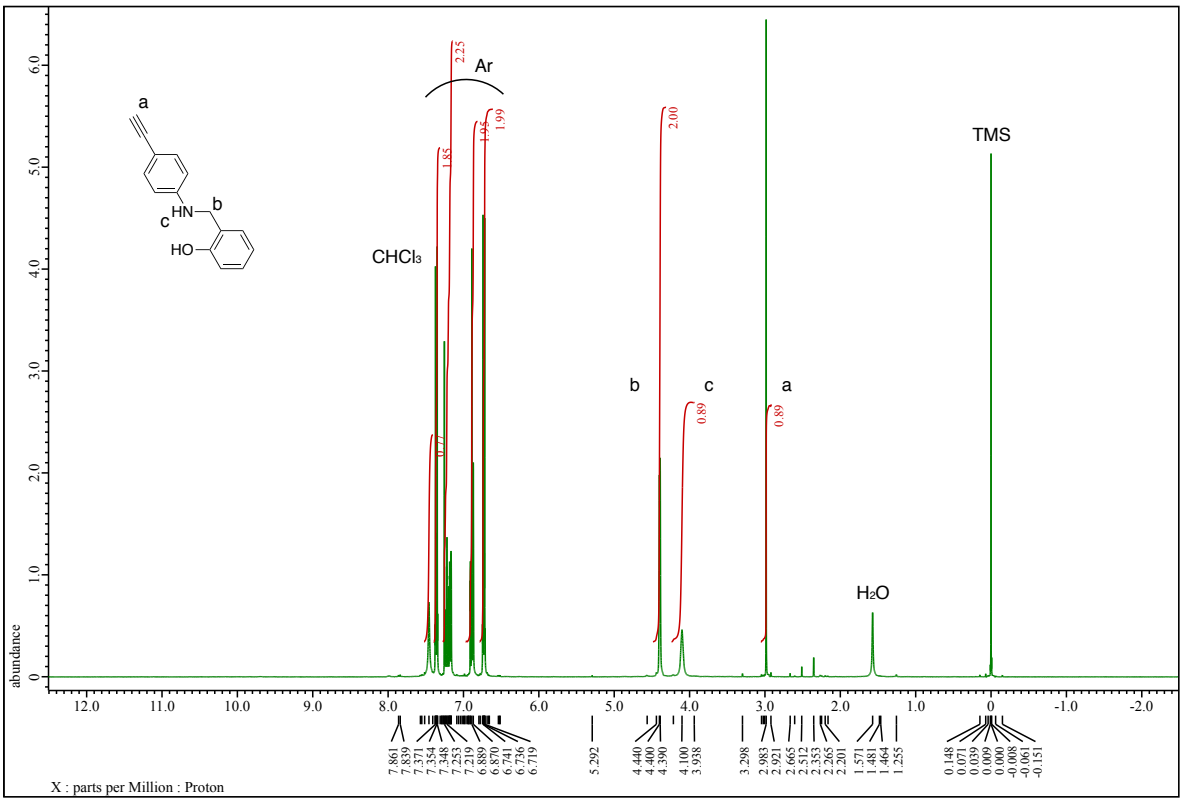

Fig. S2 ^{1}H NMR spectrum of **2** measured at 400 MHz in $CDCl_3$ at 25 °C.

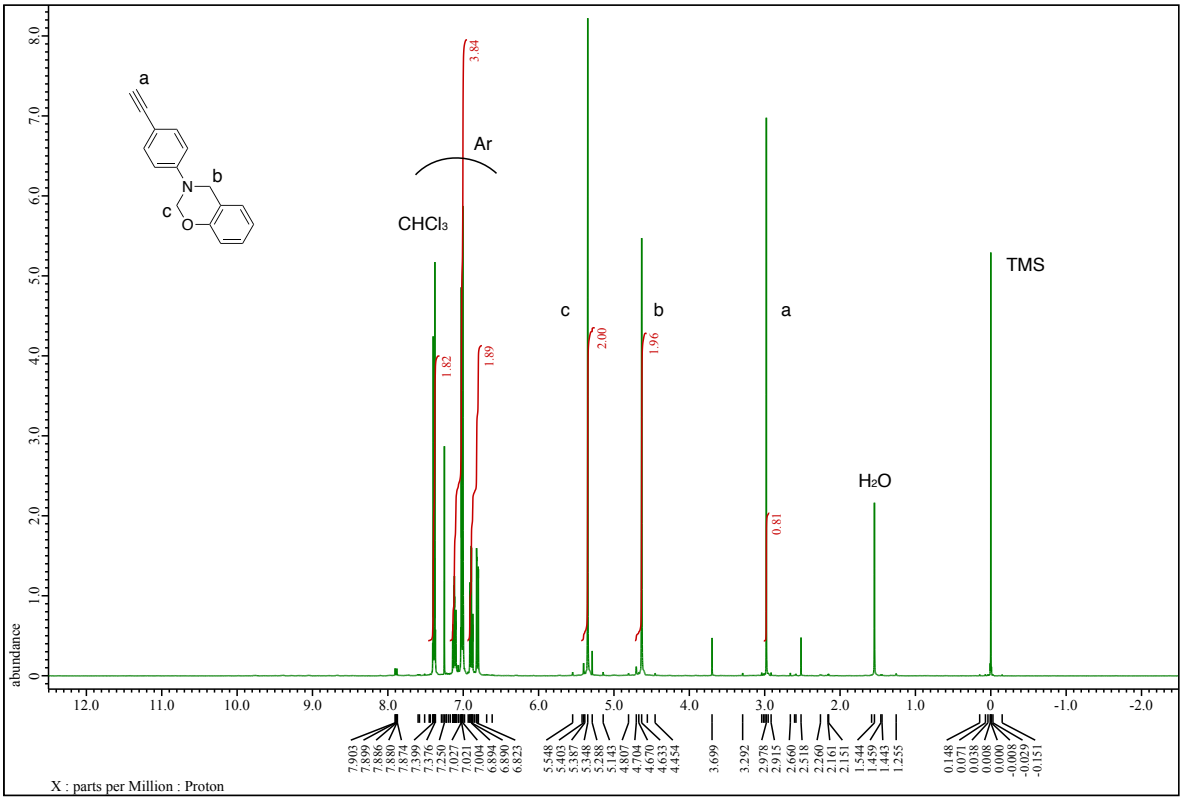

Fig. S3 ^{1}H NMR spectrum of **6** measured at 400 MHz in $CDCl_3$ at 25 °C.

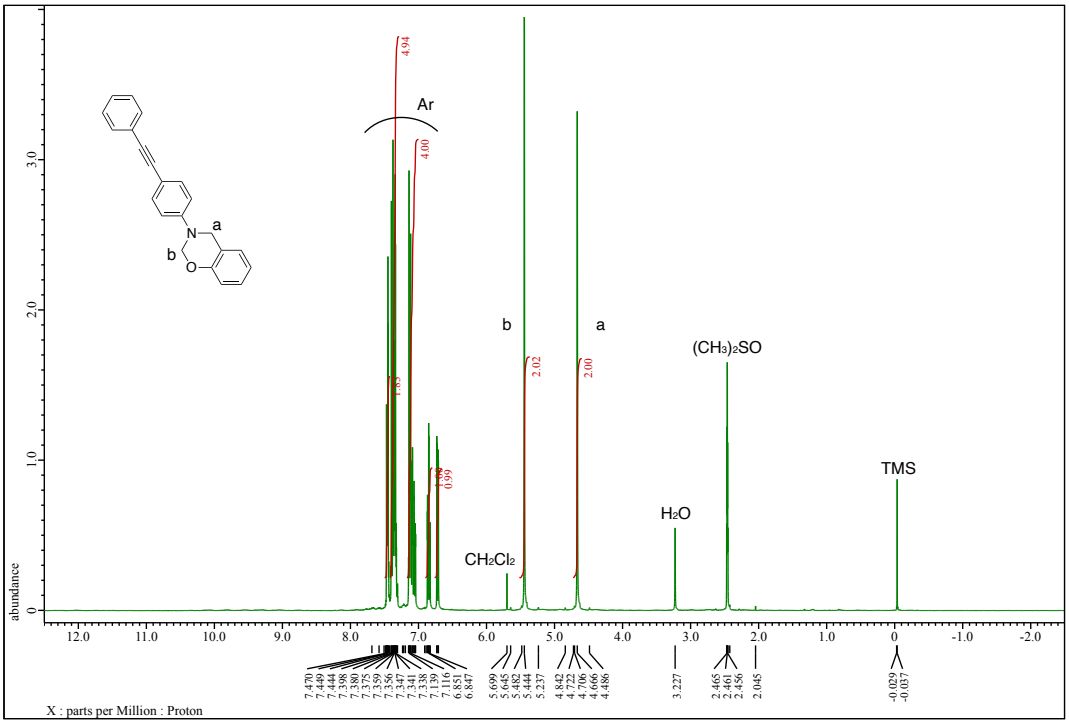

Fig. S4 ^{1}H NMR spectrum of **1** measured at 400 MHz in DMSO-d_6 at 25 °C.

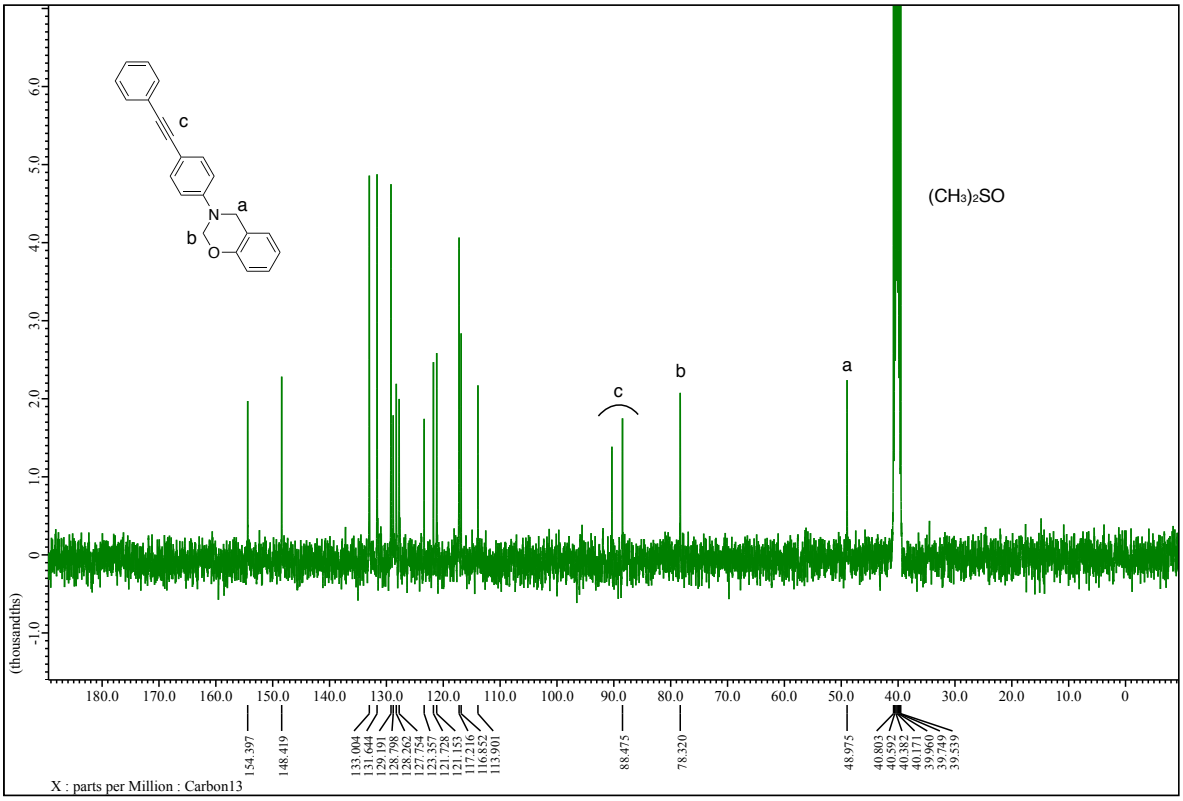

Fig. S5 ^{13}C NMR spectrum of **1** measured at 100 MHz in DMSO-d_6 at 25 °C.

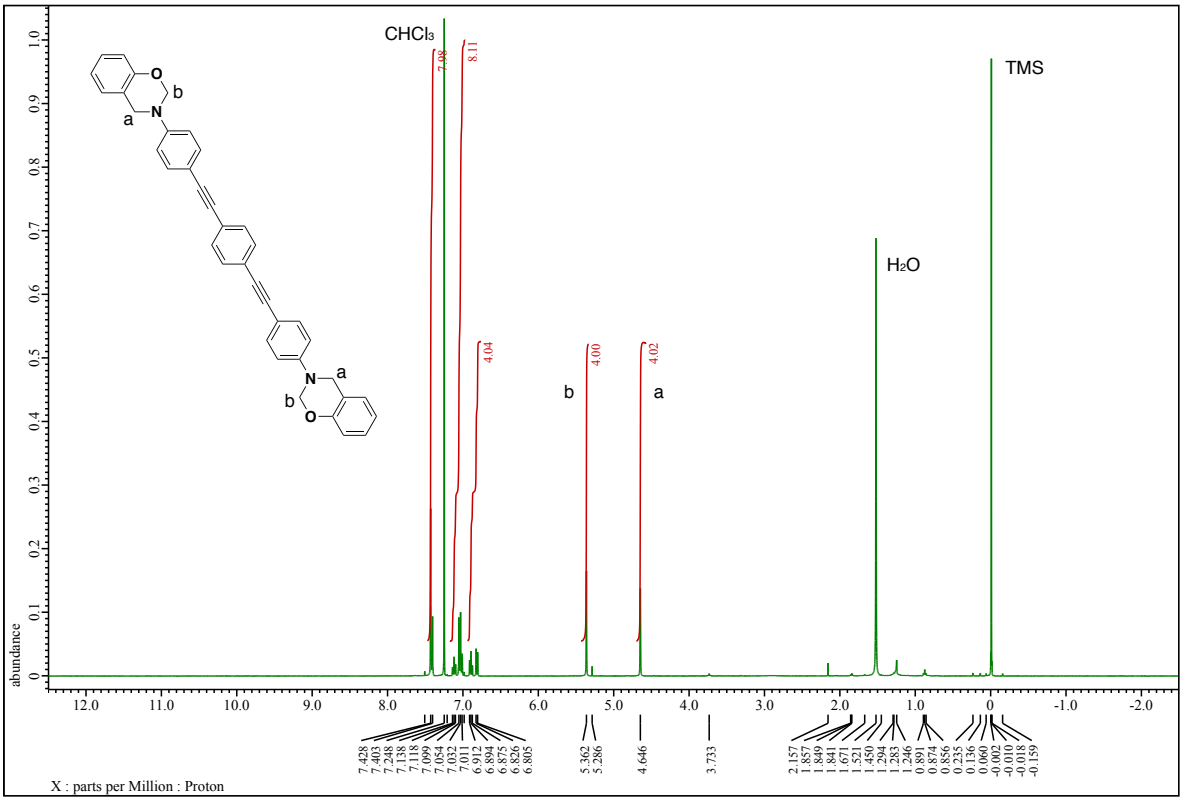

Fig. S6 ^{1}H NMR spectrum of **2** measured at 400 MHz in $CHCl_3$ at 25 °C.

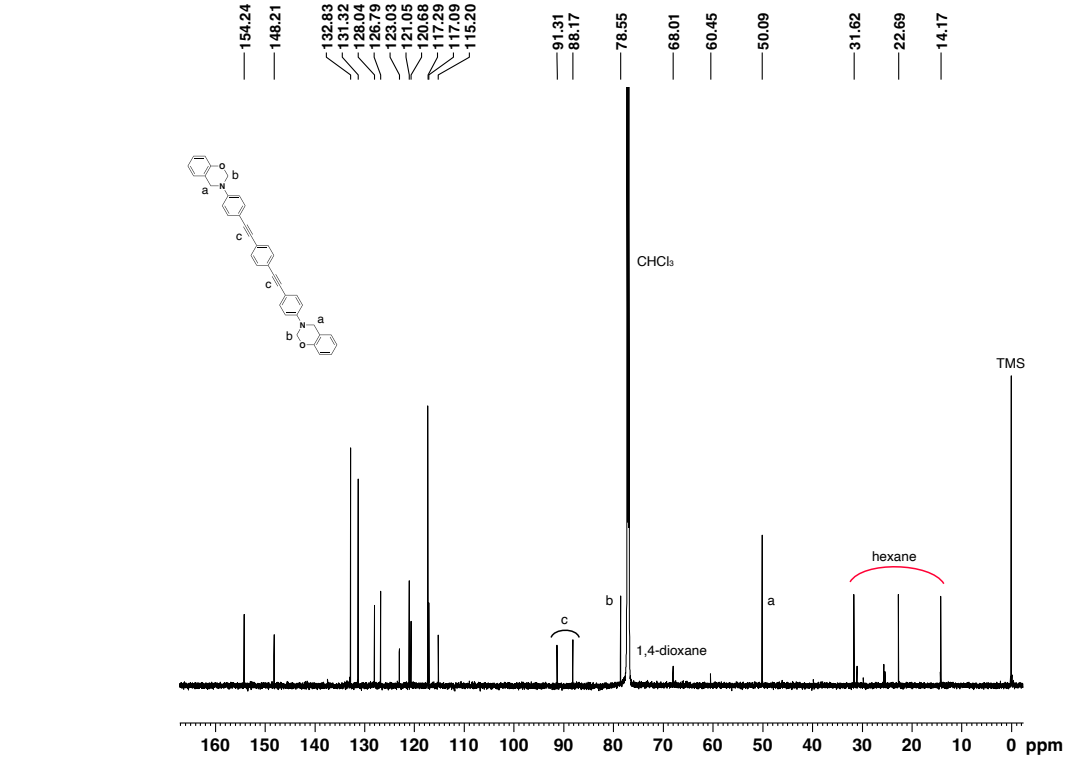

Fig. S7 ^{13}C NMR spectrum of **2** measured at 175 MHz in $CHCl_3$ at 25 °C.

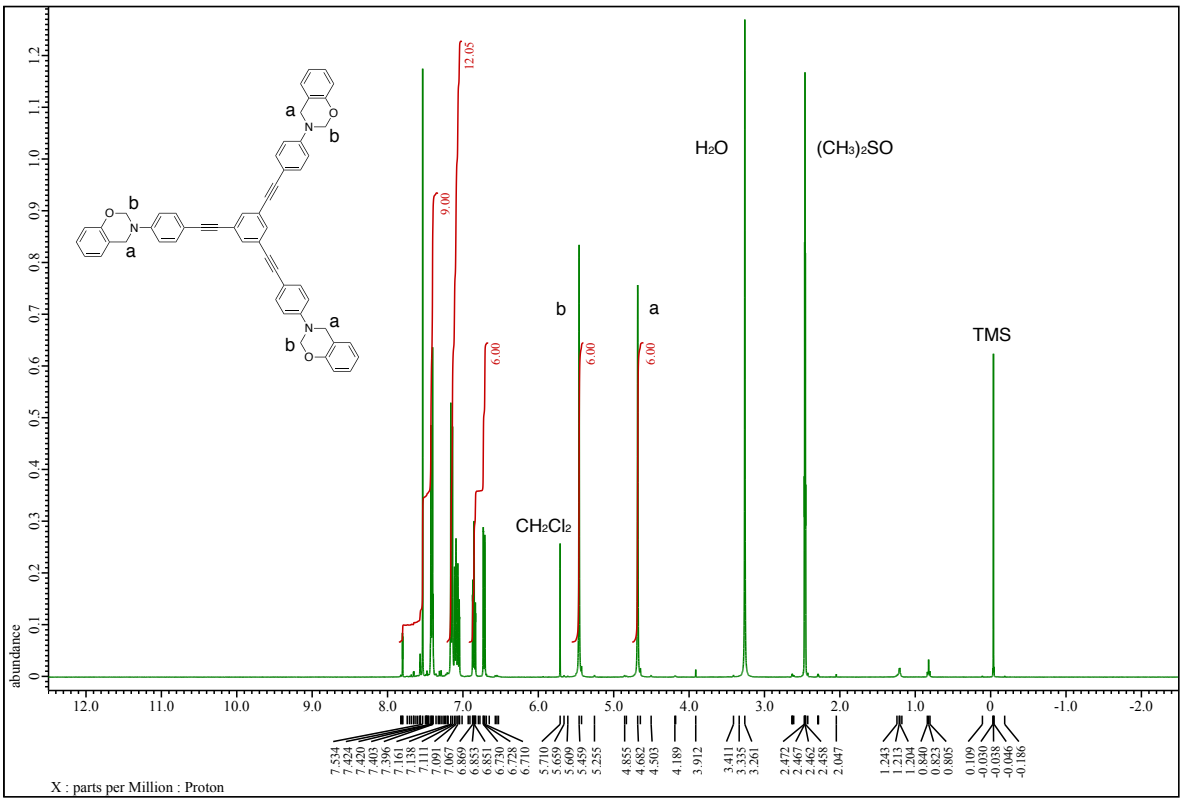

Fig. S8 ^{1}H NMR spectrum of **3** measured at 400 MHz in DMSO-d_6 at 25 °C.

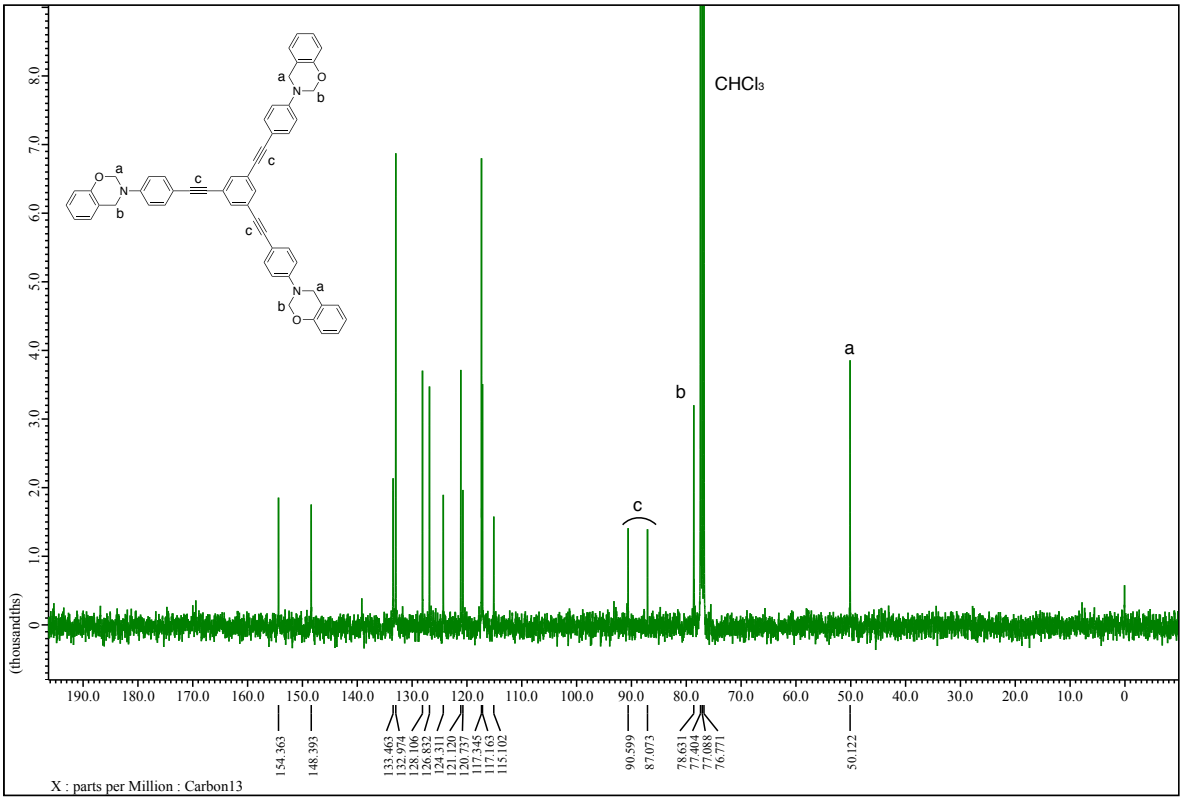

Fig. S9 ^{13}C NMR spectrum of **3** measured at 100 MHz in $CDCl_3$ at 25 °C.

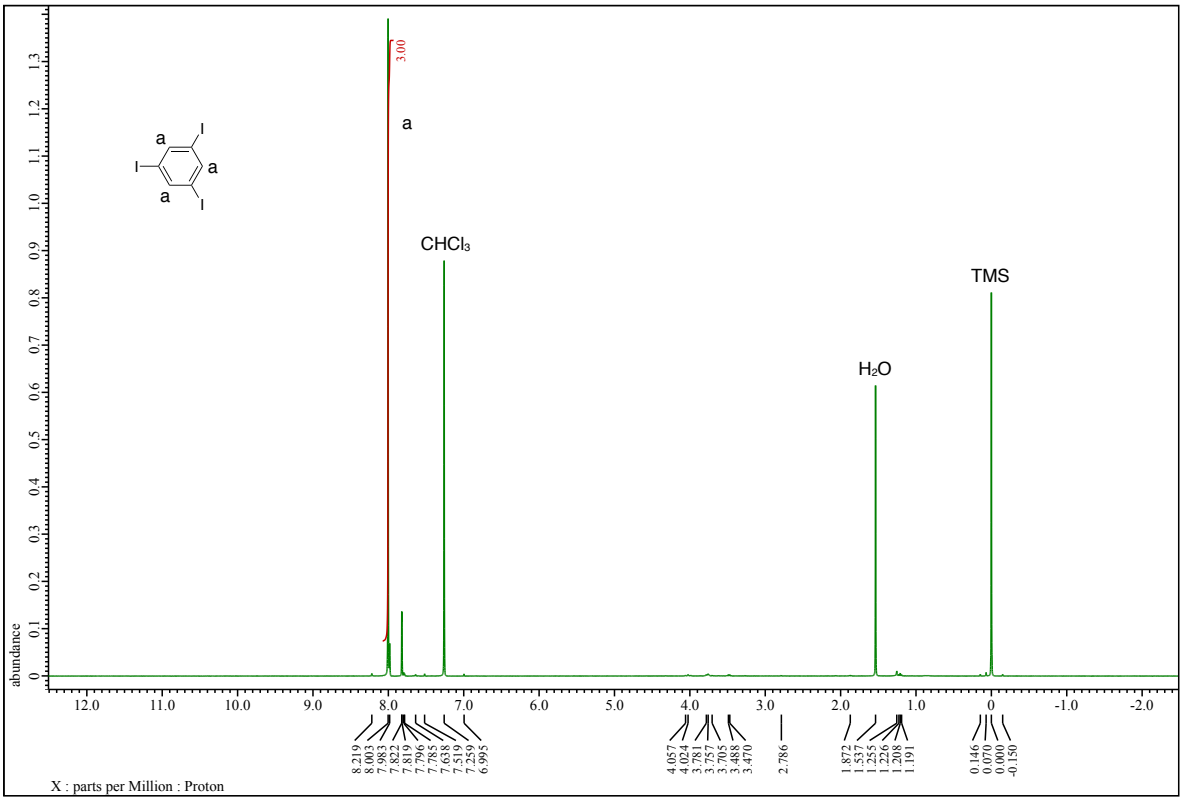

Fig. S10 ^{1}H NMR spectrum of 1,3,5-triiodobenzene measured at 100 MHz in $CDCl_3$ at 25 °C.

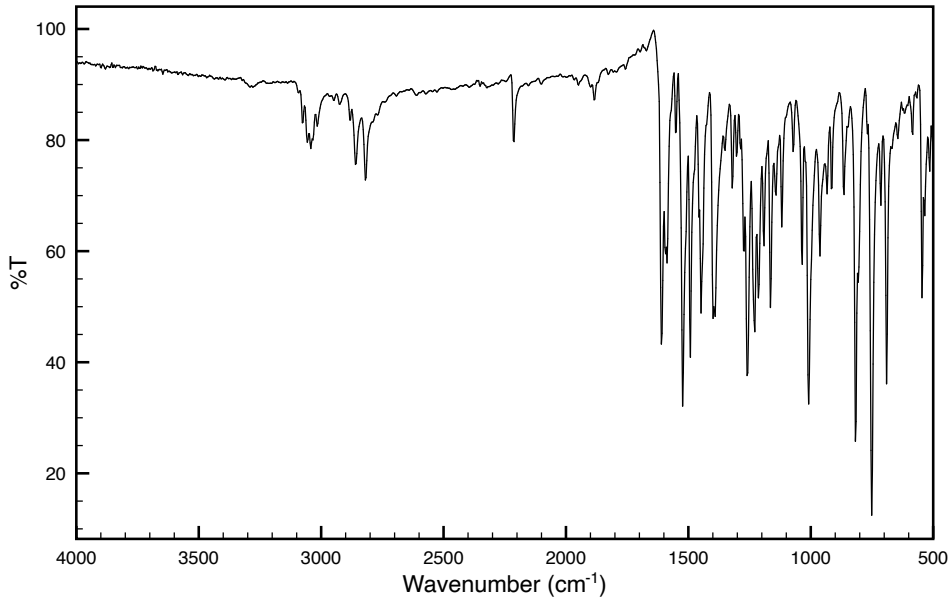

Fig. S11 IR absorption spectrum (KBr pellet) of **1**.

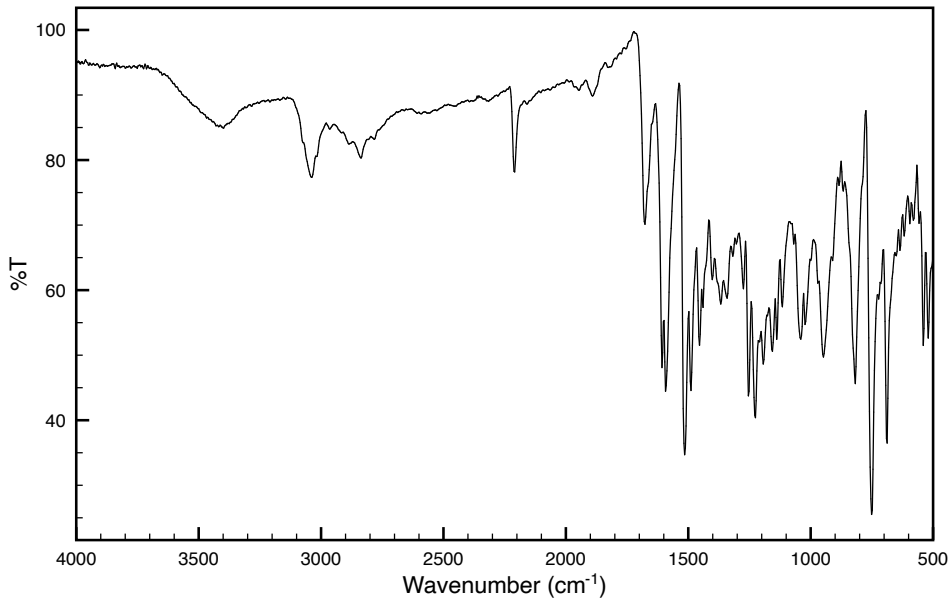

Fig. S12 IR absorption spectrum (KBr pellet) of a resin obtained by curing of **1** at 150 °C.

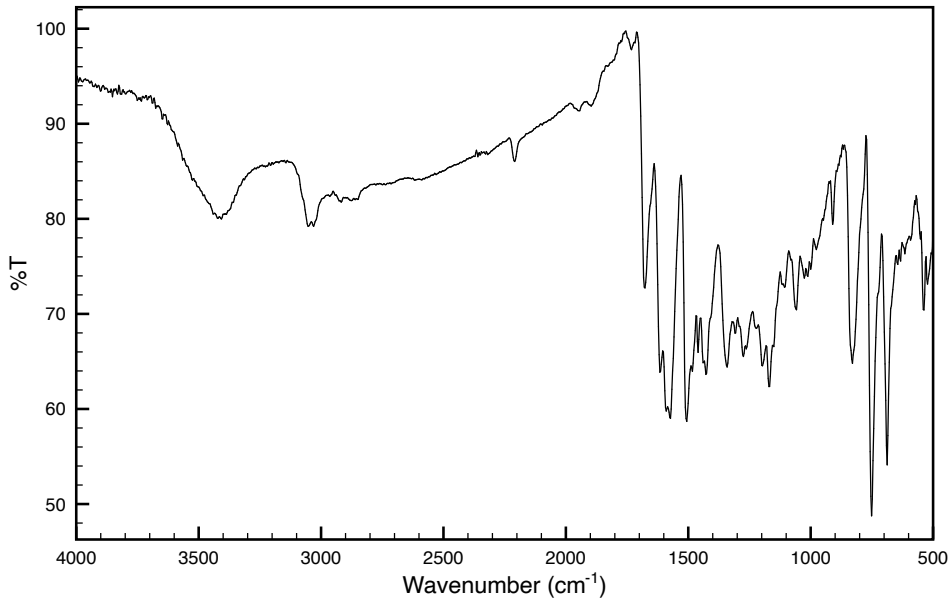

Fig. S13 IR absorption spectrum (KBr pellet) of a resin obtained by curing of **1** at 200 °C.

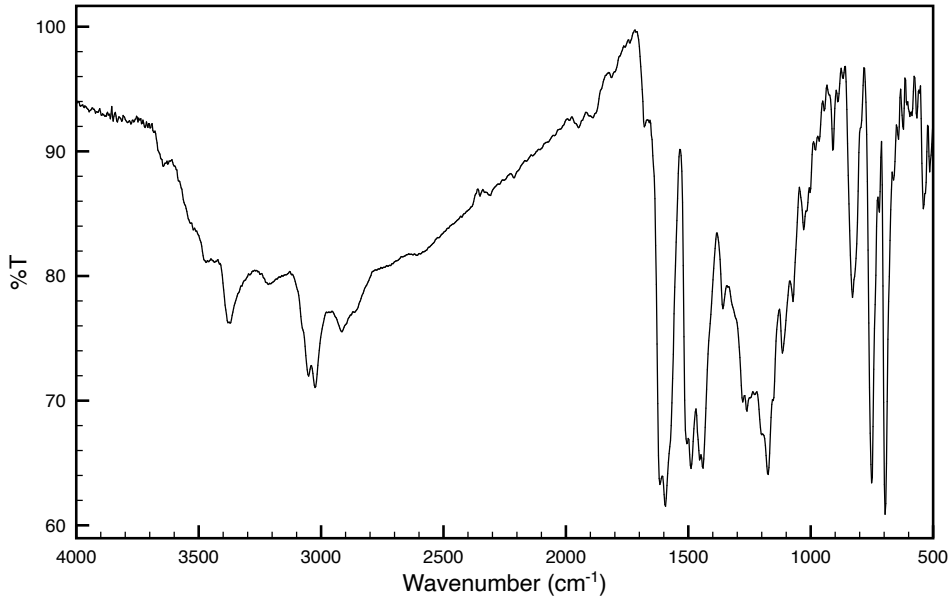

Fig. S14 IR absorption spectrum (KBr pellet) of a resin obtained by curing of **1** at 250 °C.

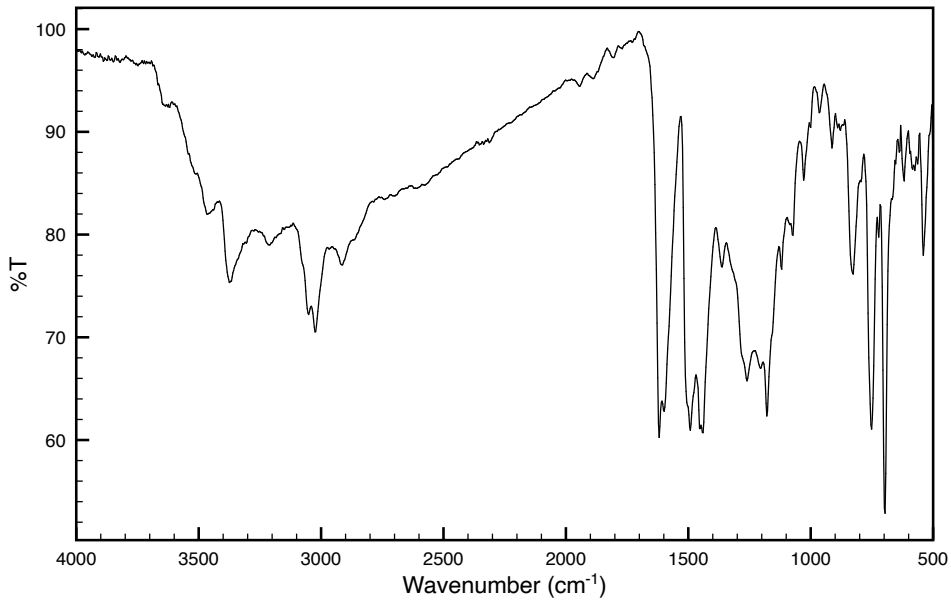

Fig. S15 IR absorption spectrum (KBr pellet) of a resin obtained by curing of **1** at 300 °C.

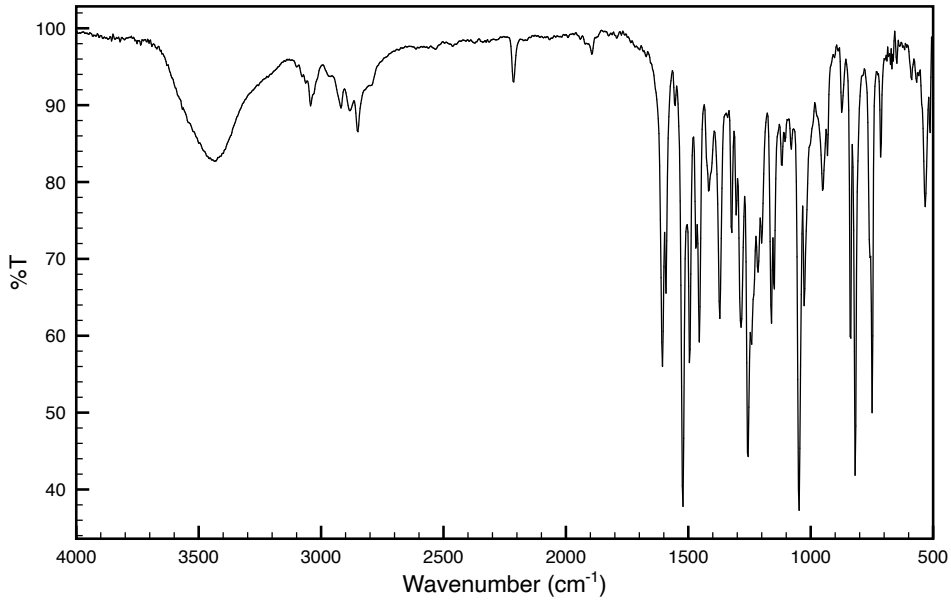

Fig. S16 IR absorption spectrum (KBr pellet) of **2**.

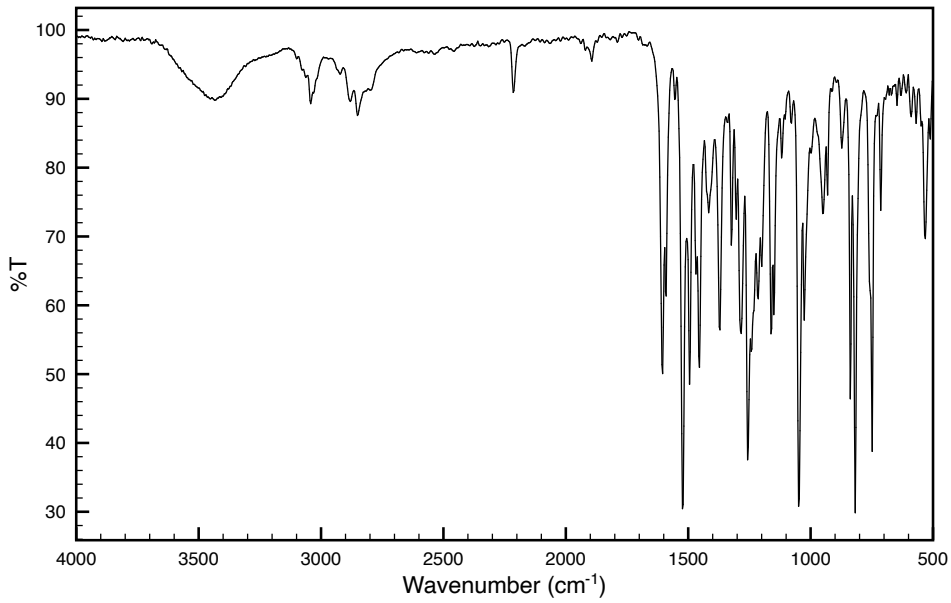

Fig. S17 IR absorption spectrum (KBr pellet) of a resin obtained by curing of **2** at 150 °C.

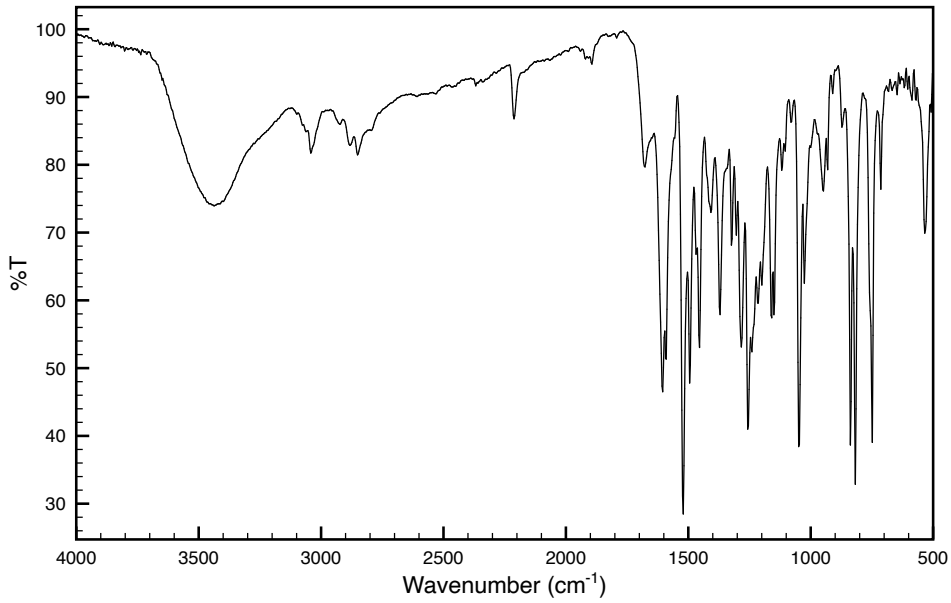

Fig. S18 IR absorption spectrum (KBr pellet) of a resin obtained by curing of **2** at 200 °C.

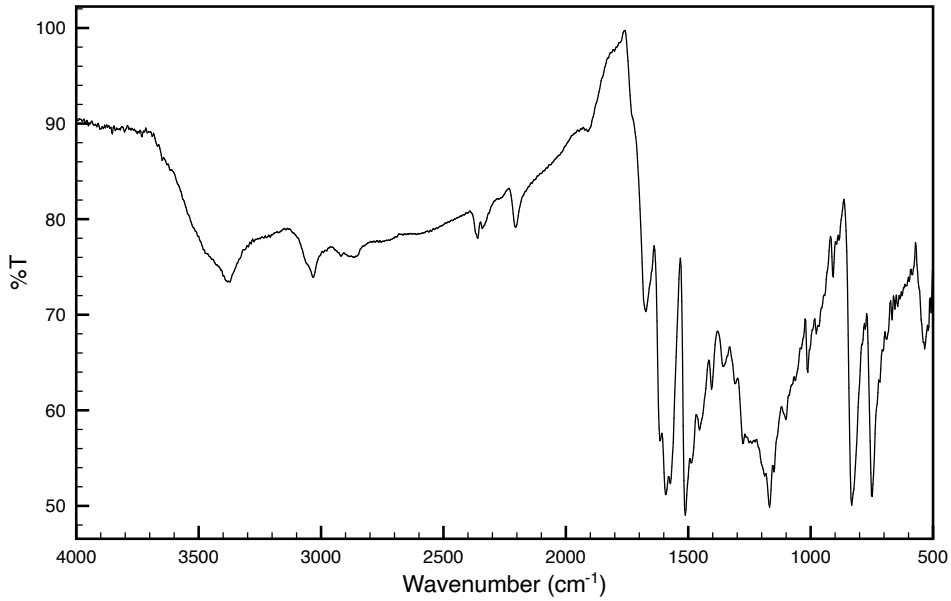

Fig. S19 IR absorption spectrum (KBr pellet) of a resin obtained by curing of **2** at 250 °C.

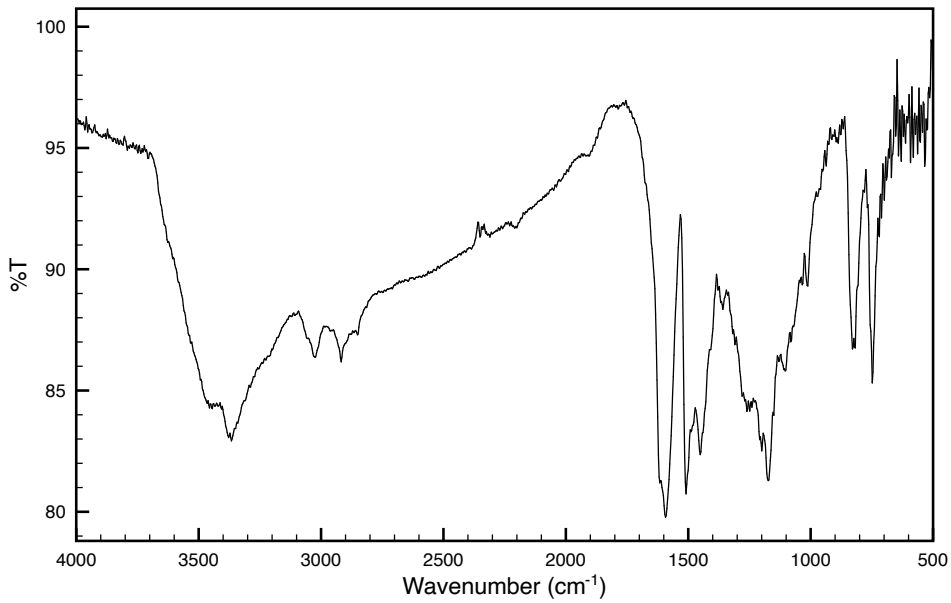

Fig. S20 IR absorption spectrum (KBr pellet) of a resin obtained by curing of **2** at 300 °C.

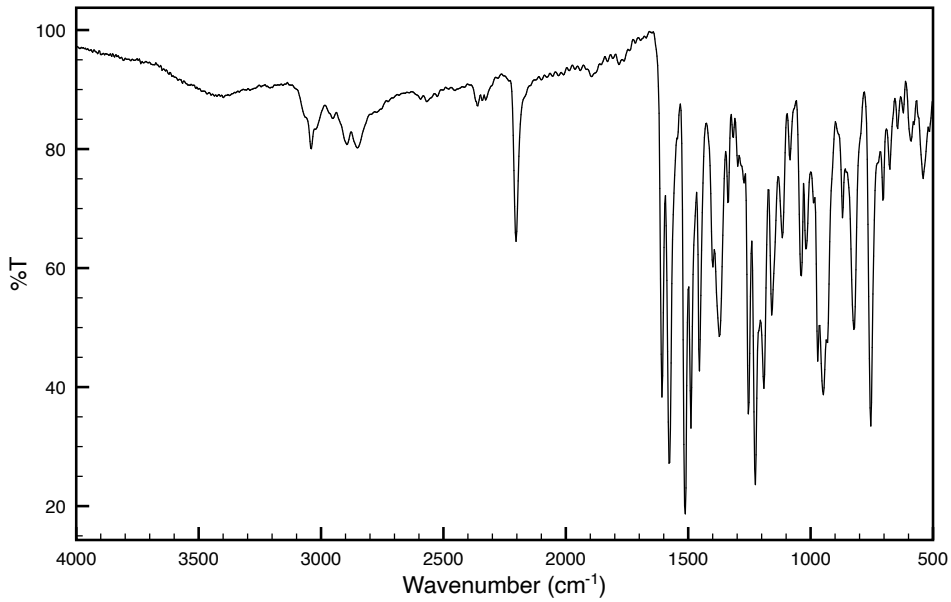

Fig. S21 IR absorption spectrum (KBr pellet) of **3**.

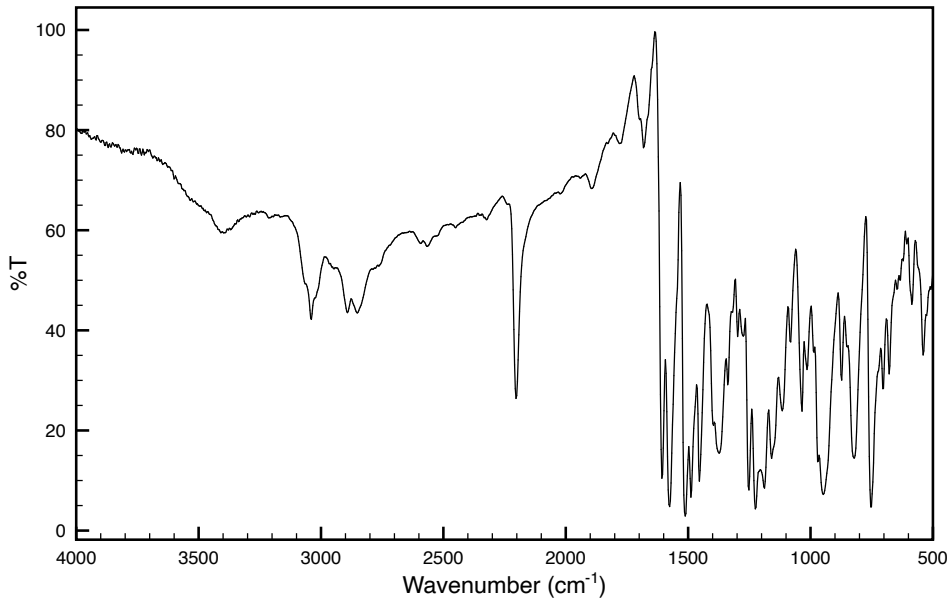

Fig. S22 IR absorption spectrum (KBr pellet) of a resin obtained by curing of **3** at 150 °C.

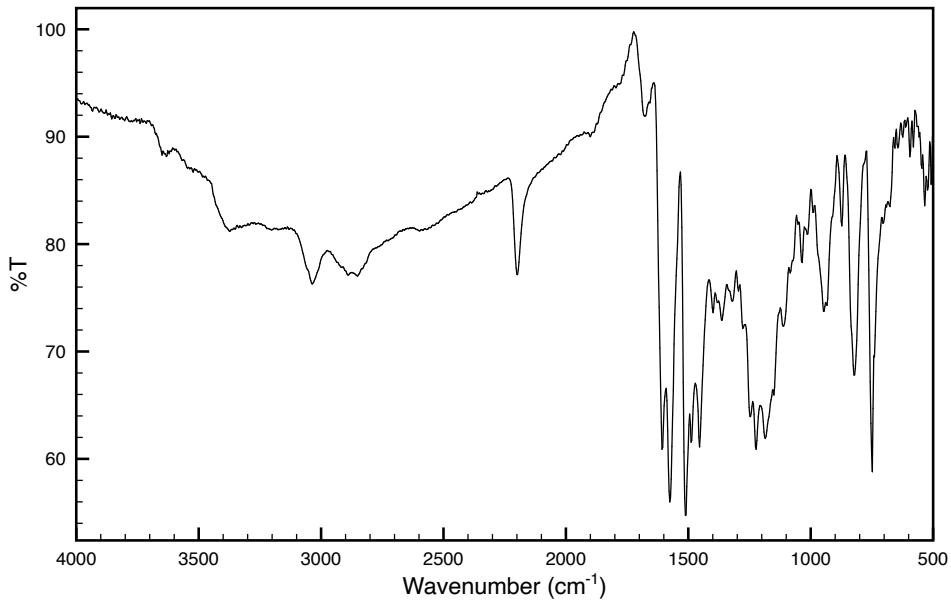

Fig. S23 IR absorption spectrum (KBr pellet) of a resin obtained by curing of **3** at 200 °C.

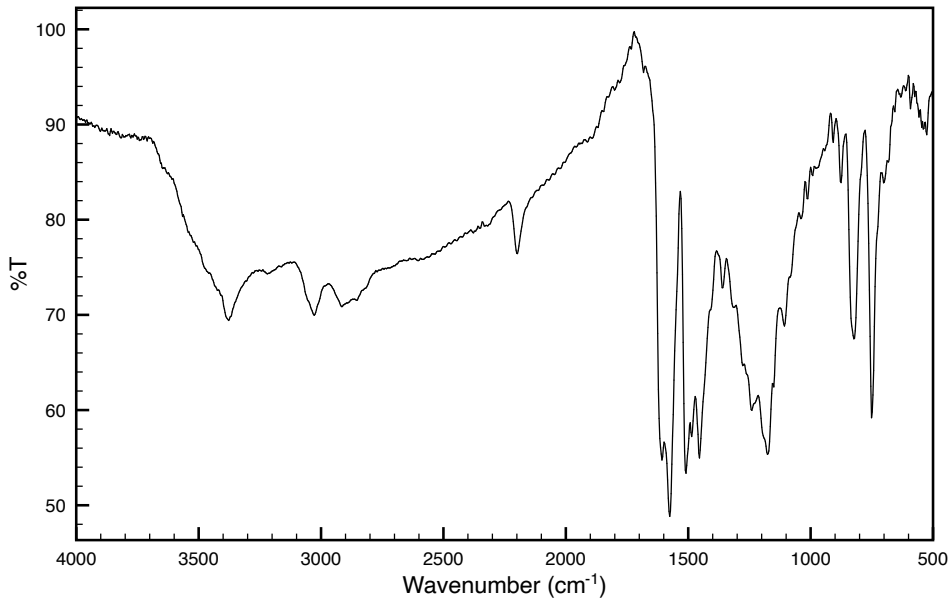

Fig. S24 IR absorption spectrum (KBr pellet) of a resin obtained by curing of **3** at 250 °C.

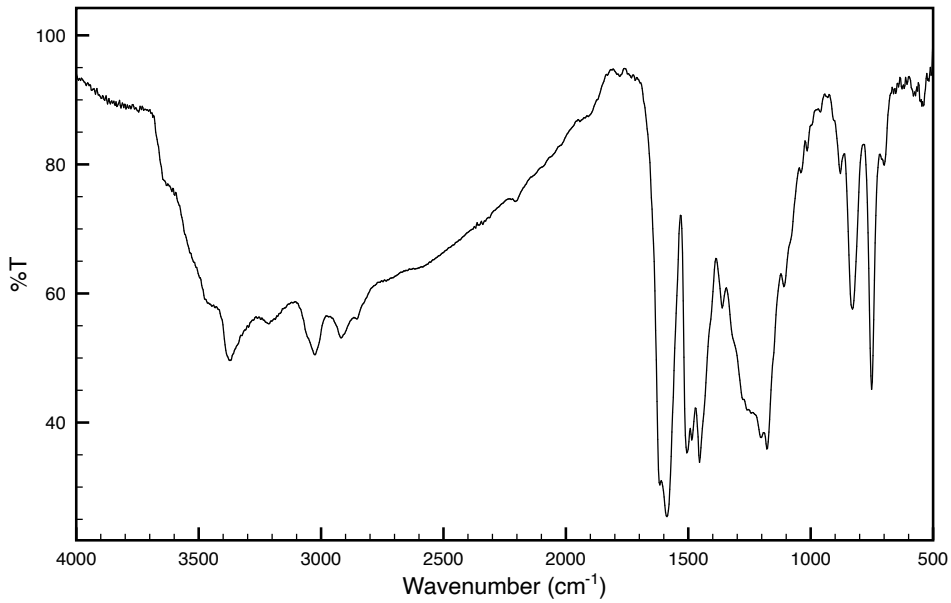

Fig. S25 IR absorption spectrum (KBr pellet) of a resin obtained by curing of **3** at 300 °C.

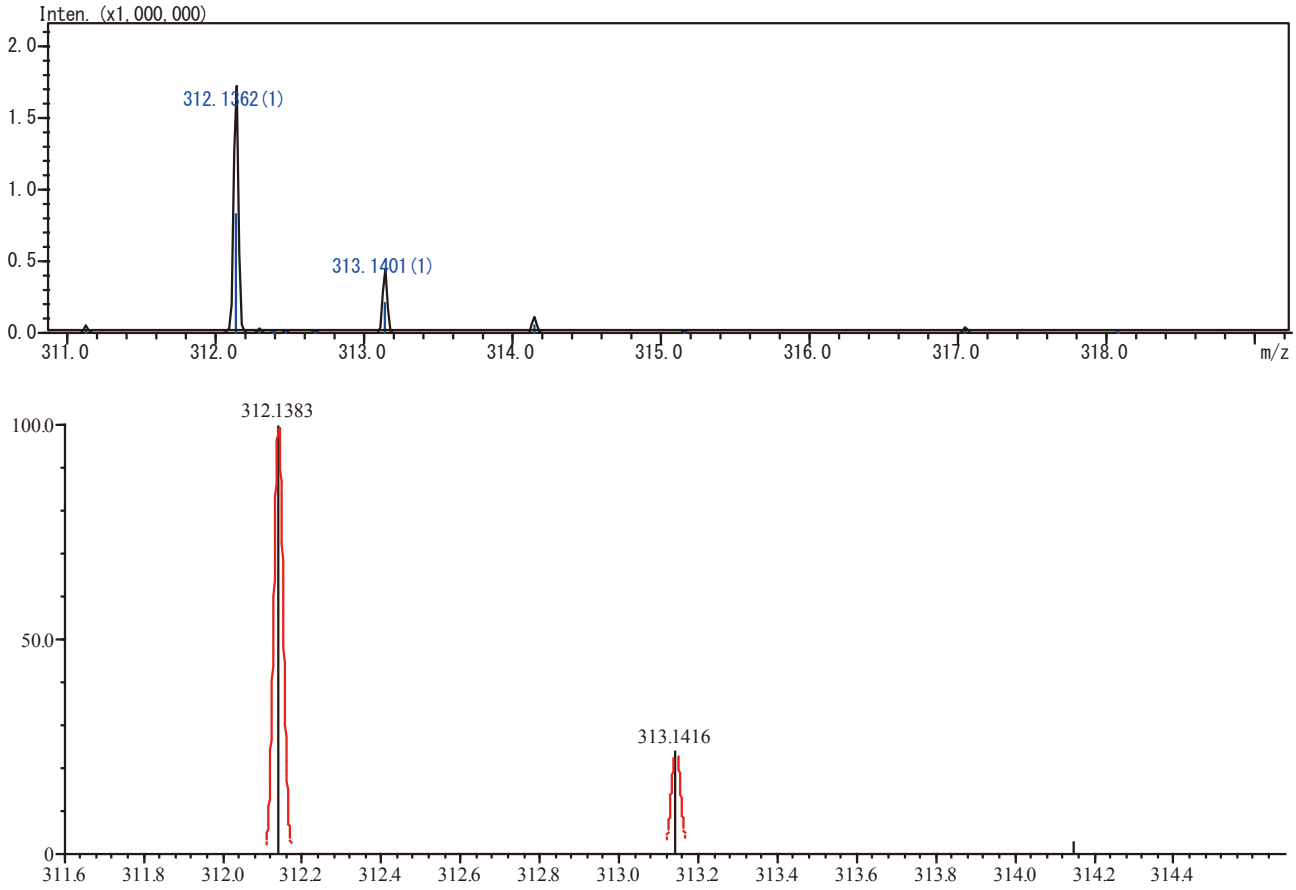

Fig. S26 ESI-TOF-MS of **1**; (top) found, (bottom) calcd.

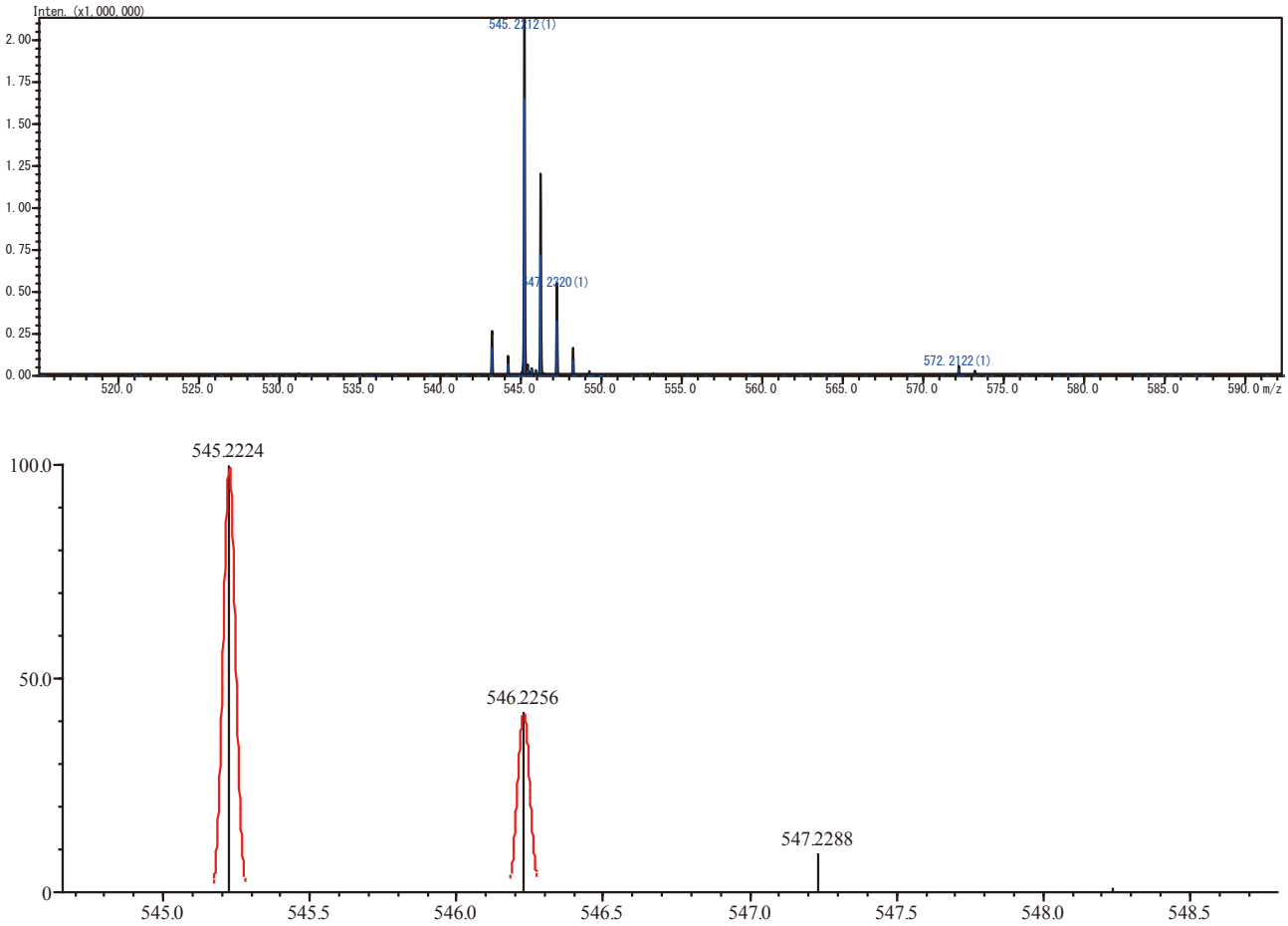

Fig. S27 ESI-TOF-MS of **2**; (top) found, (bottom) calcd.

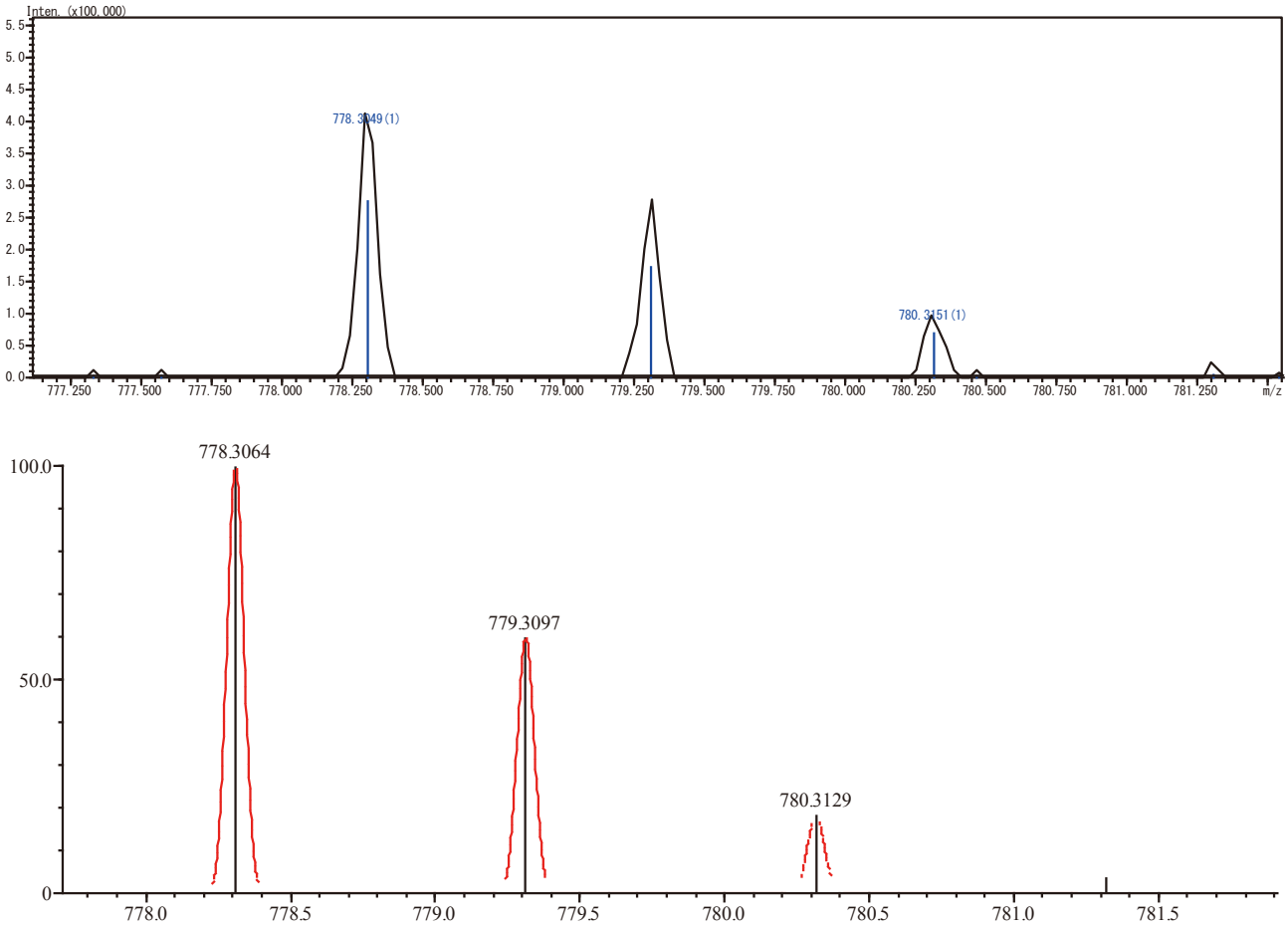

Fig. S28 ESI-TOF-MS of **3**; (top) found, (bottom) calcd.

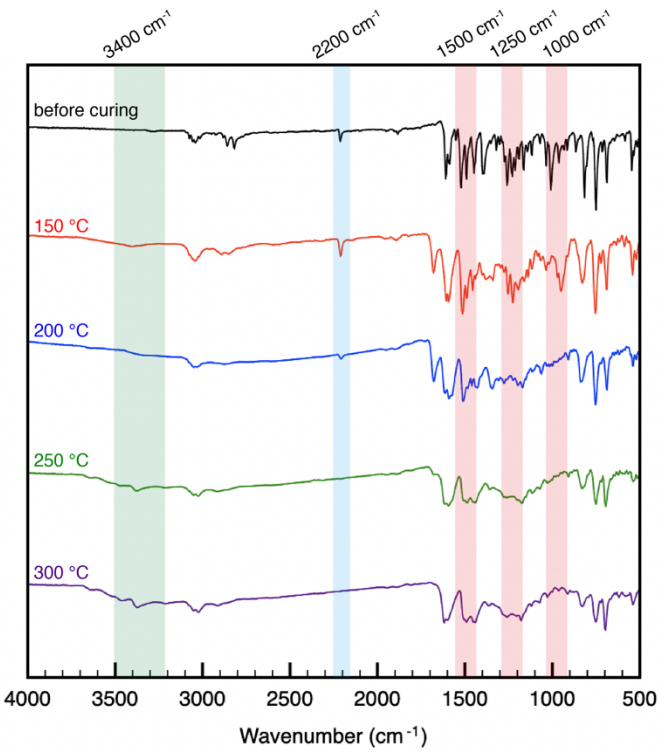

Fig. S29 IR absorption spectra of **1** and resins obtained by curing of **1** at 150–300 °C for 2 h. The peak at 1650 cm^{-1} is assignable to C=N bond in the Schiff base structure formed during the ring-opening process.[S16]

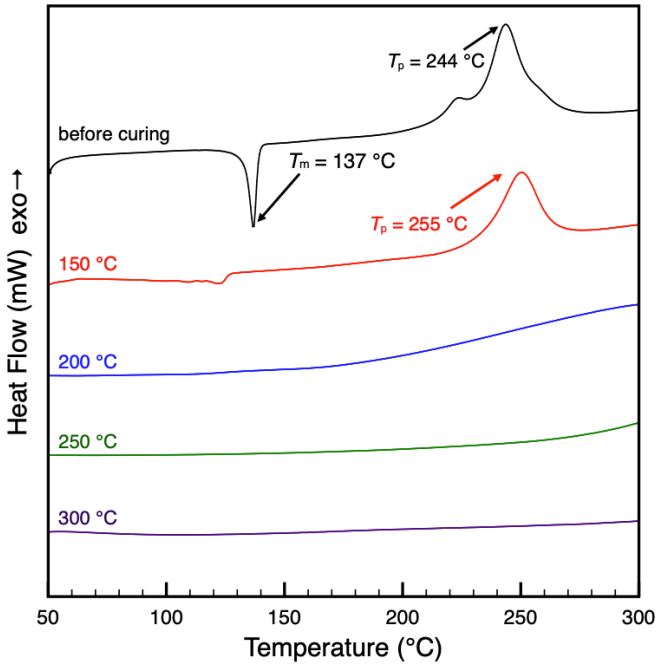

Fig. S30 DSC thermograms of **1** and resins obtained by curing of **1** at 150–300 °C for 2 h.

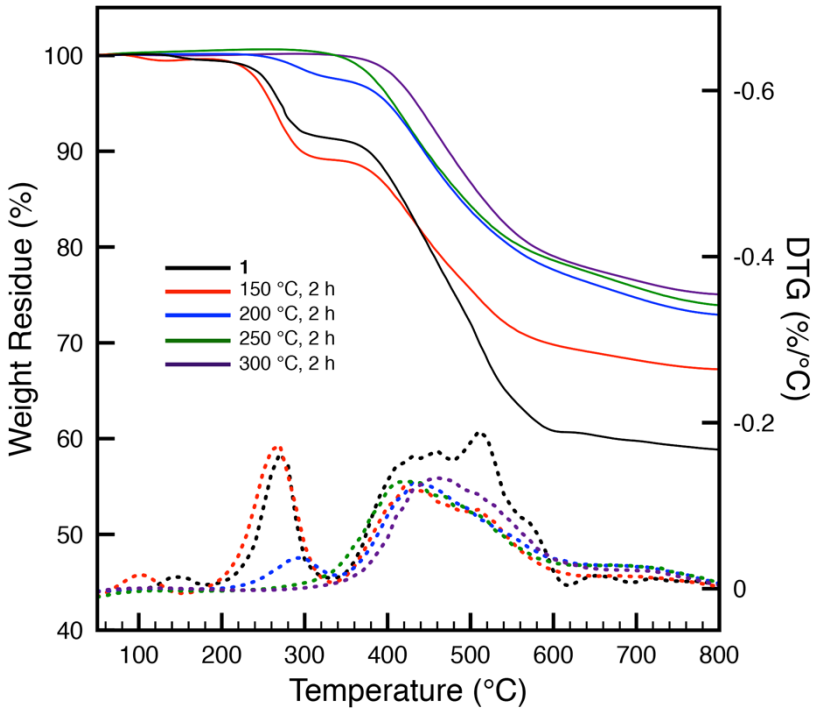

Fig. S31 TGA traces and DTG (dashed line) of **1** and resins obtained by curing of **1** at 150–300 °C for 2 h.

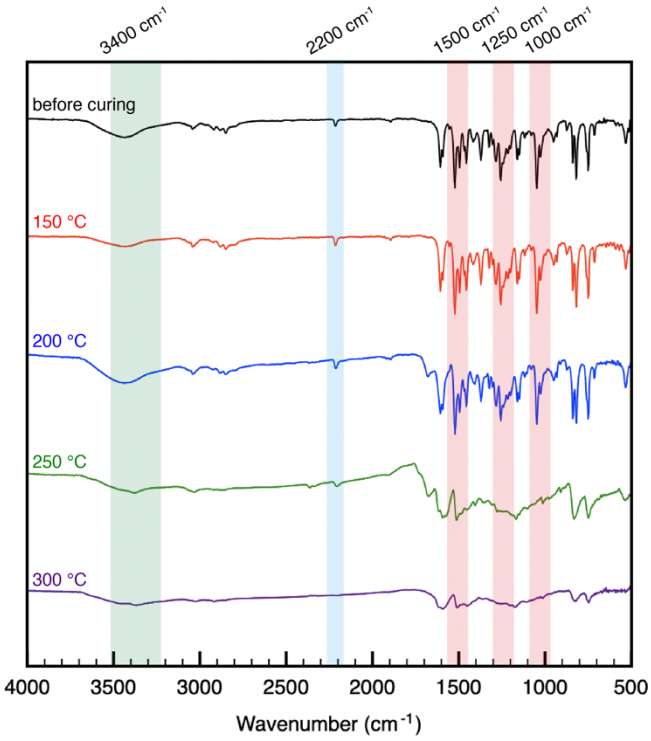

Fig. S32 IR absorption spectra of **2** and resins obtained by curing of **2** at 150–300 °C for 2 h. The peak at 1650 cm^{-1} is assignable to C=N bond in the Schiff base structure formed during the ring-opening process.[S16]

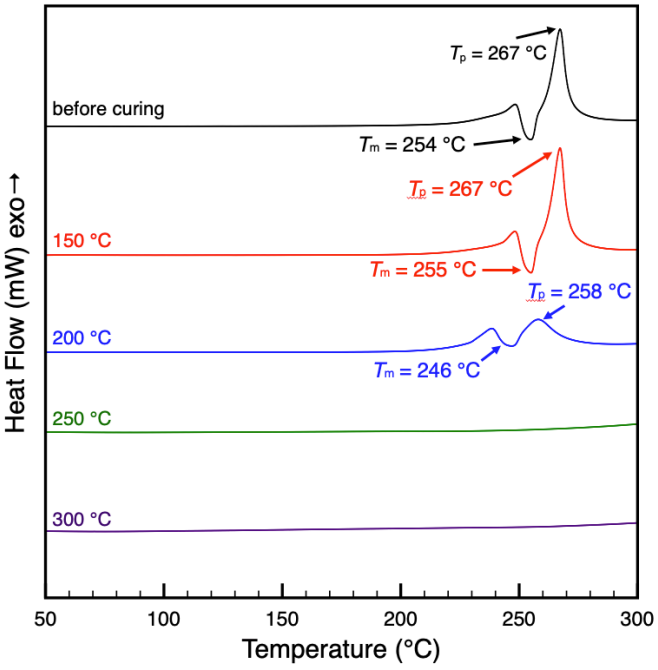

Fig. S33 DSC thermograms of **2** and resins obtained by curing of **2** at 150–300 °C for 2 h.

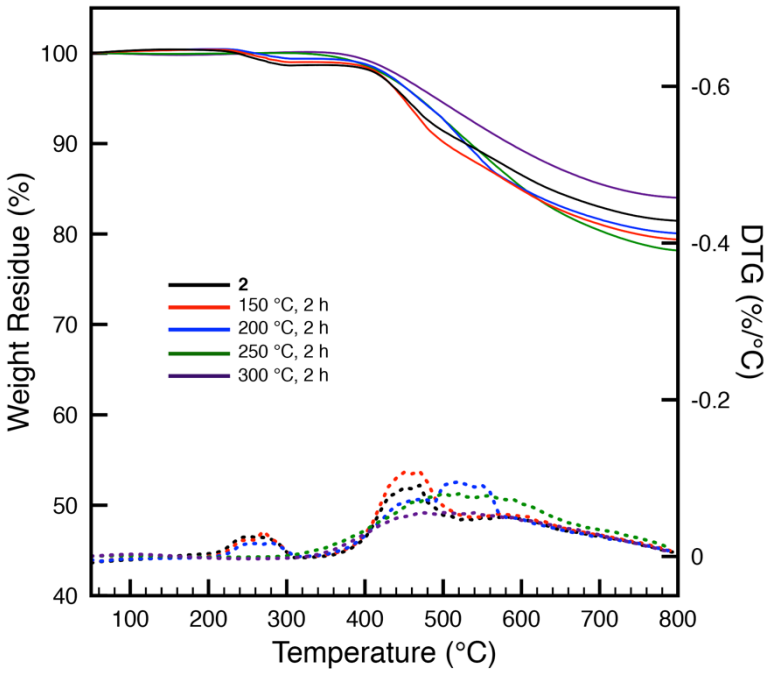

Fig. S34 TGA traces and DTG (dashed line) of **2** and resins obtained by curing of **2** at 150–300 °C for 2 h.

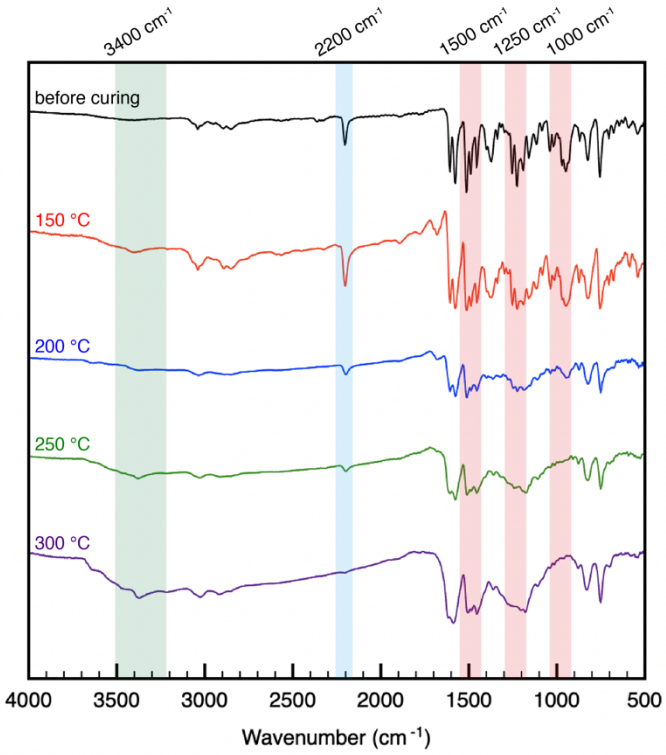

Fig. S35 IR absorption spectra of **3** and resins obtained by curing of **3** at 150–300 °C for 2 h. The peak at 1650 cm^{-1} is assignable to C=N bond in the Schiff base structure formed during the ring-opening process.[S16]

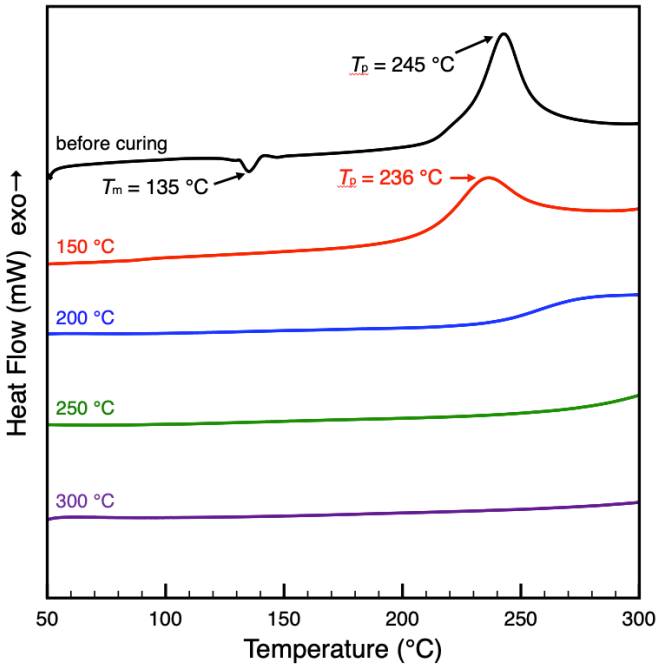

Fig. S36 DSC thermograms of **3** and resins obtained by curing of **3** at 150–300 °C for 2 h.

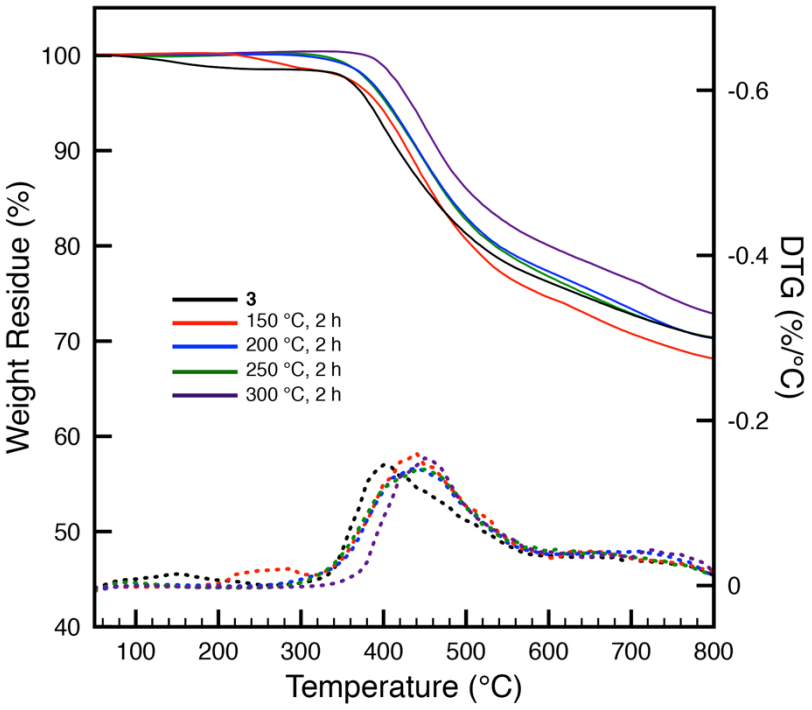

Fig. S37 TGA traces and DTG (dashed line) of **3** and resins obtained by curing of **3** at 150–300 °C for 2 h.

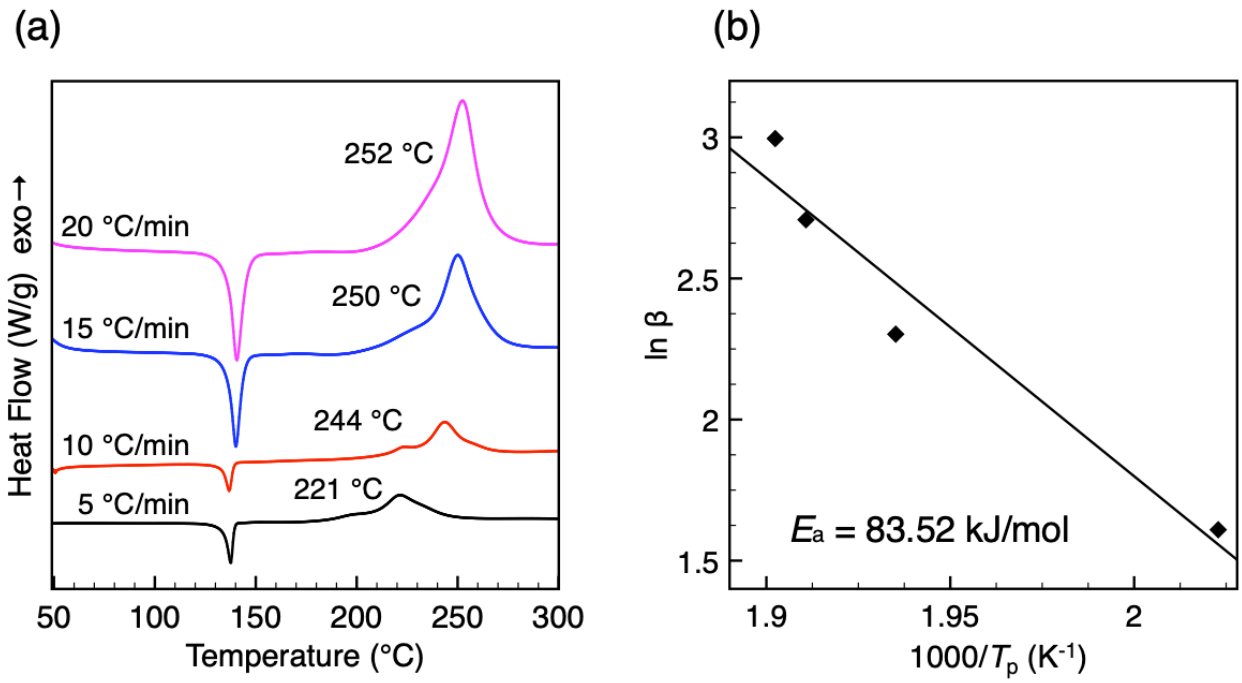

Fig. S38 (a) DSC thermograms of **1** at various heating rates. (b) Ozawa–Flynn–Wall plot for the data of (a). Correlation coefficient r = 0.9408.

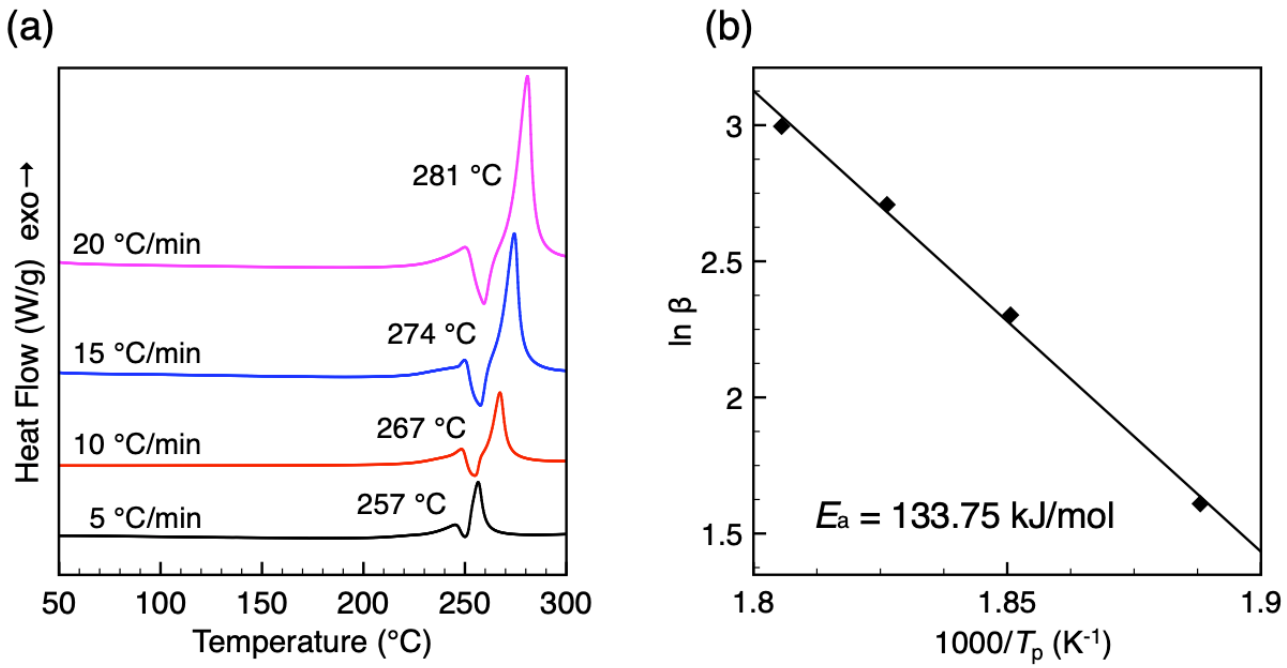

Fig. S39 (a) DSC thermograms of **2** at various heating rates. (b) Ozawa–Flynn–Wall plot for the data of (a). Correlation coefficient r = 0.9964.

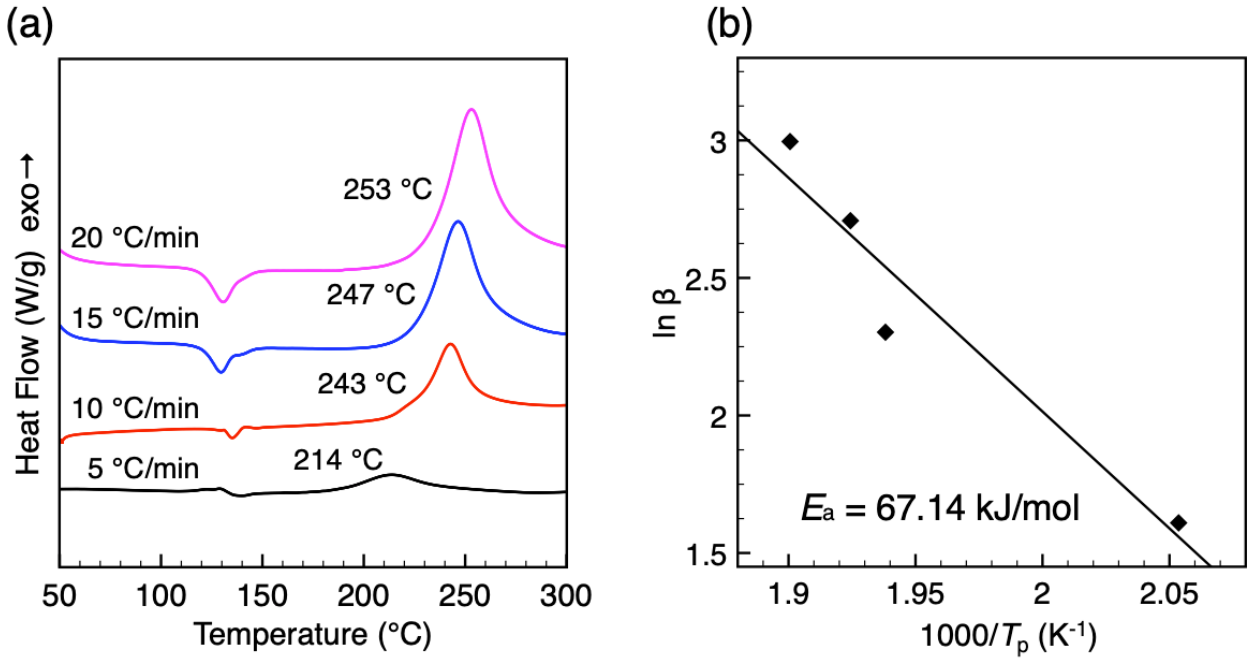

Fig. S40 (a) DSC thermograms of **3** at various heating rates. (b) Ozawa–Flynn–Wall plot for the data of (a). Correlation coefficient r = 0.9261.

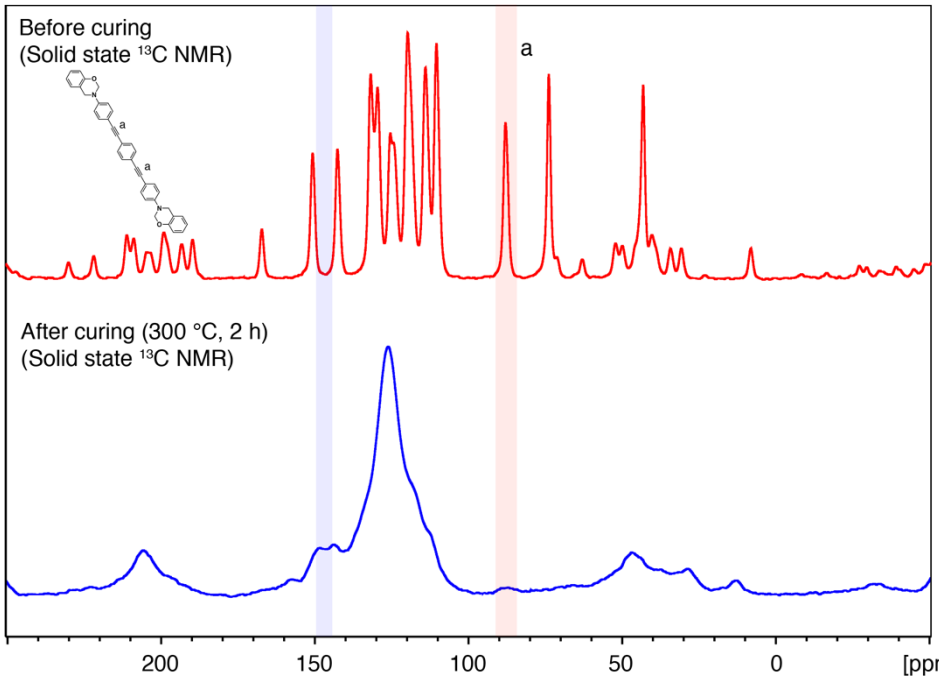

Fig. S41 ^{13}C CP/MAS NMR spectra of **2** (top) and resin obtained by curing of **2** at 300 °C (bottom).

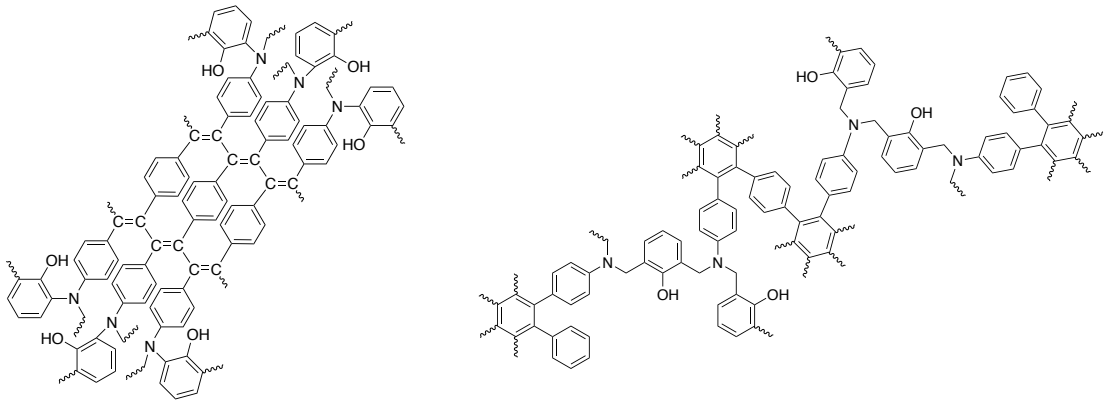

Fig. S42 Deduced structures of **2** (left) and resin formed by curing of **2** (right).

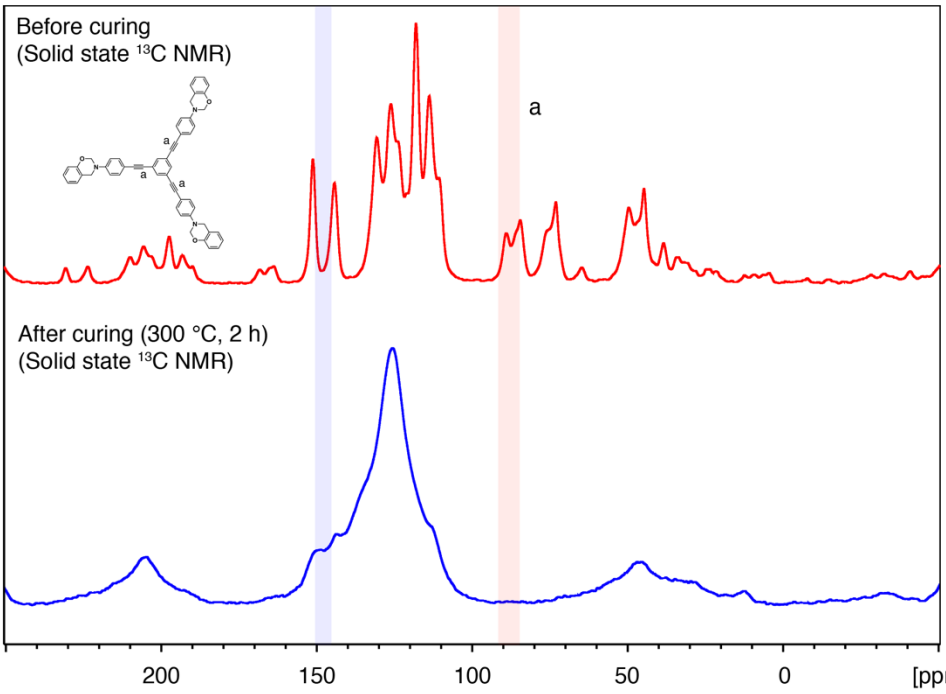

Fig. S43 ^{13}C CP/MAS NMR spectra of **3** (top) and resin obtained by curing of **3** at 300 °C (bottom).

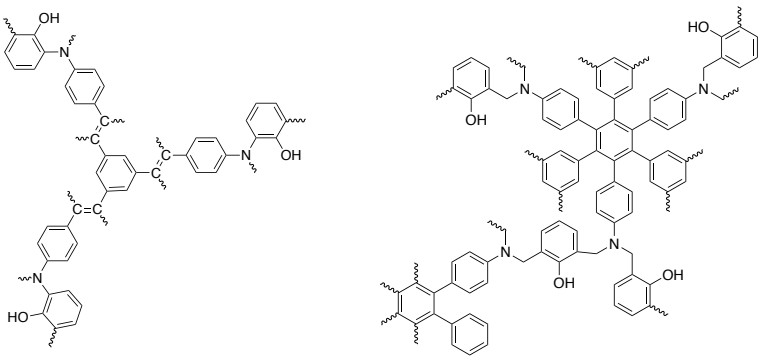

Fig. S44 Deduced structures of **3** (left) and resin formed by curing of **3** (right)

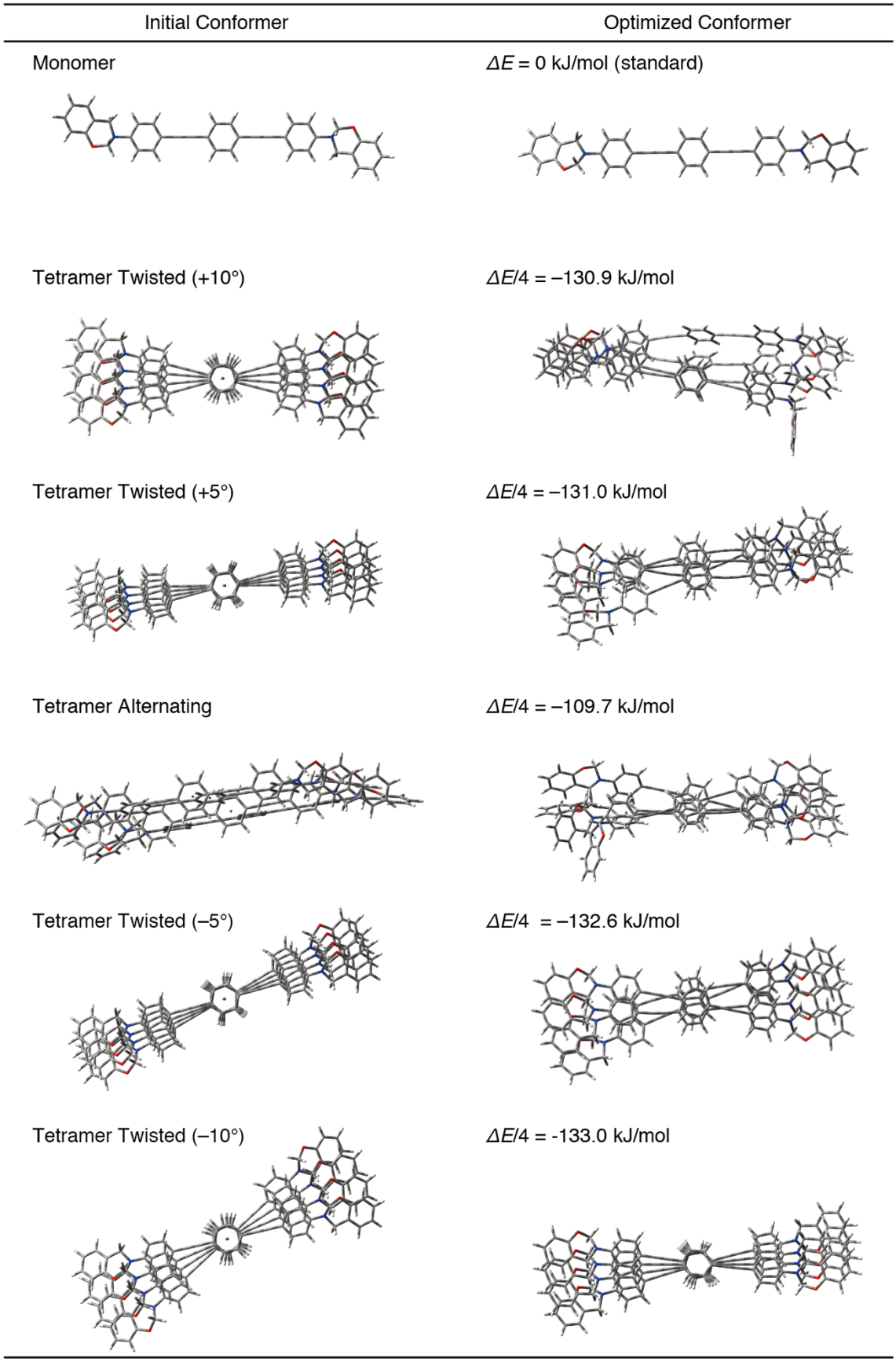

Fig. S45 Initial and DFT (ωB97X-D/6-31G*)-optimized conformers of monomeric and tetrameric molecular models of **2**.

Initial Conformer	Optimized Conformer
Monomer	ΔE = 0 kJ/mol (standard)
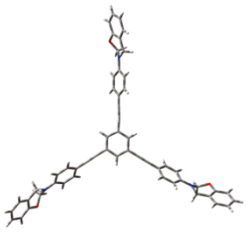	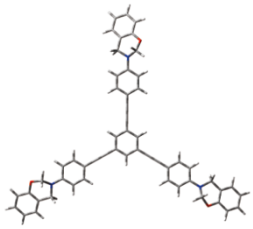
Tetramer Twisted (+20°)	ΔE/4 = -192.1 kJ/mol
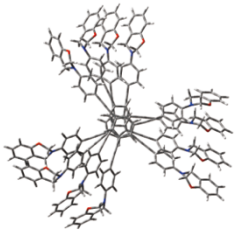	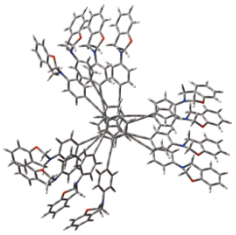
Tetramer Twisted (+15°)	ΔE/4 = –200.8 kJ/mol
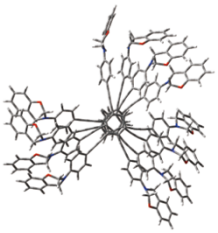	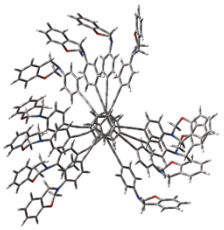
Tetramer Twisted (+10°)	ΔE/4 = –193.8 kJ/mol
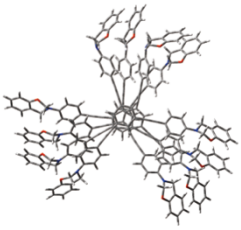	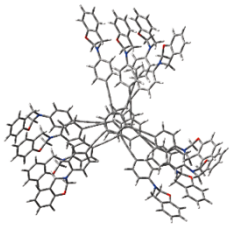
Tetramer Twisted (–15°)	ΔE/4 = –112.1 kJ/mol
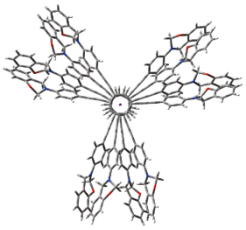	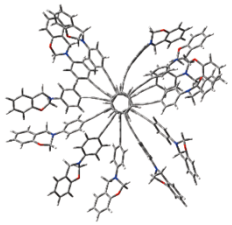
Tetramer Twisted (–20°)	ΔE/4 = –114.6 kJ/mol
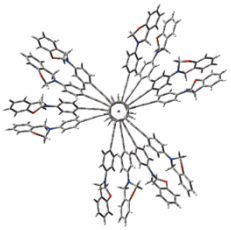	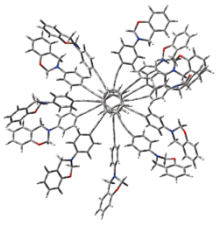

Fig. S46 Initial and DFT (ωB97X-D/6-31G*)-optimized conformers of monomeric and tetrameric molecular models of **3**.

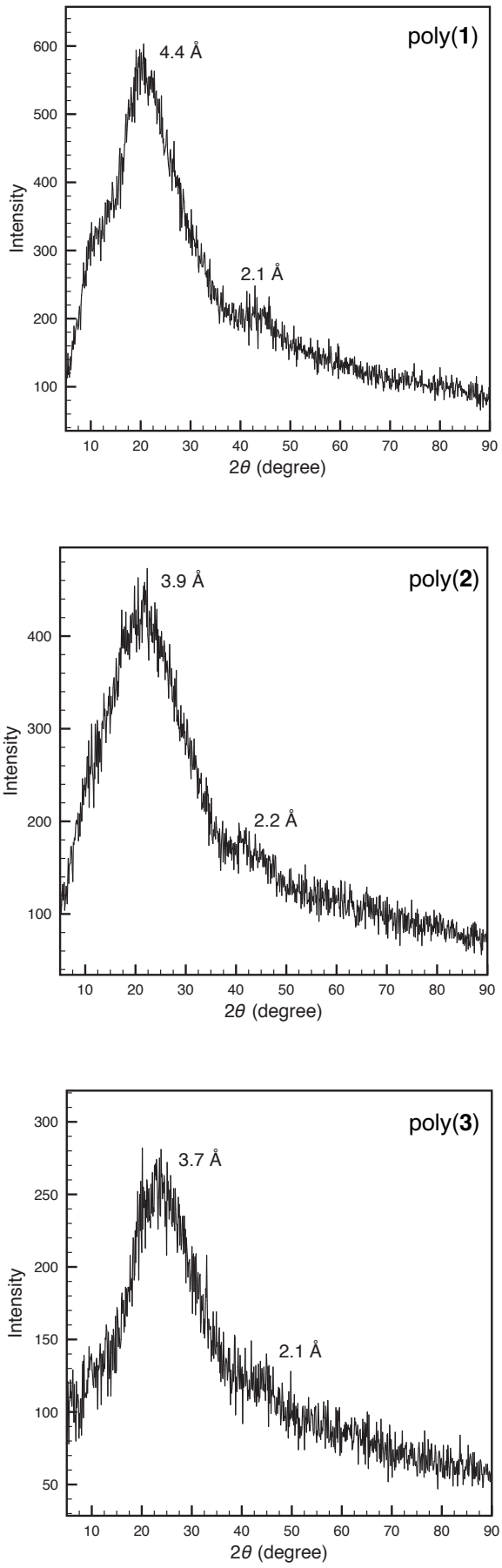

Fig. S47 Powder XRD patterns of poly(**1**)–poly(**3**) with Cu-Kα radiation.

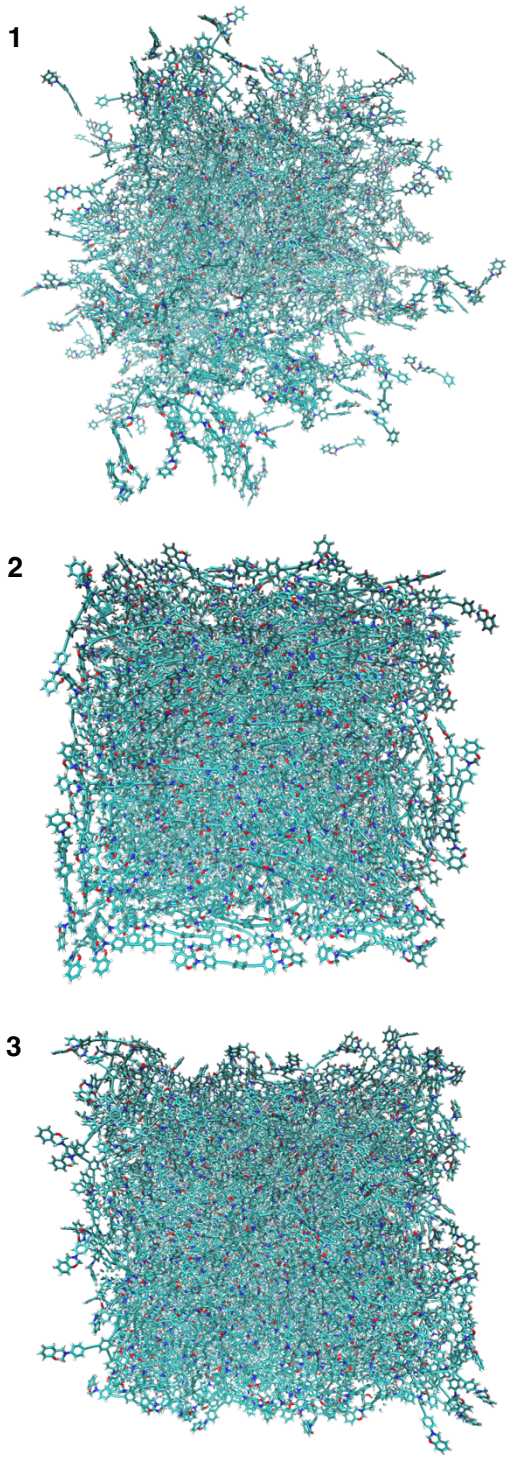

Fig. S48 Snapshots of trajectories of MD simulation of **1**–**3** at 5 ns, 300 K using models consisting of 1000 molecules by LAMMPS 2020.[S13] The densities of benzoxazines **1**, **2** and **3** were calculated to be 1.285, 1.313 and 1.264, respectively (average values of a period of 4–5 ns simulated for 1,000 ns). Also see trajectory movies in the Supporting Information.

Table S1 Observed and MD simulated densities of **1**–**3**

Compound	Density (g/cm^3)	
	Observed [a]	MD simulated [b]
1	1.285	1.126
2	1.313	1.158
3	1.264	1.154

[a] Average of 10 measurements by gas pycnometry at 26 °C. [b] Average value of a period of 4–5 ns simulated for 1,000 molecules at 300 K with LAMMPS 2020.[S13]

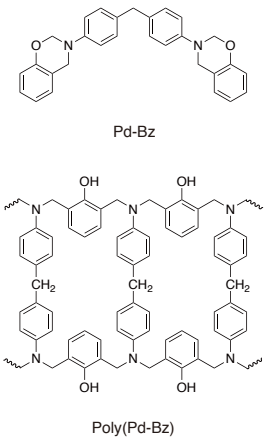

Fig. S49 Chemical structures of Pd-Bz and poly(Pd-Bz).

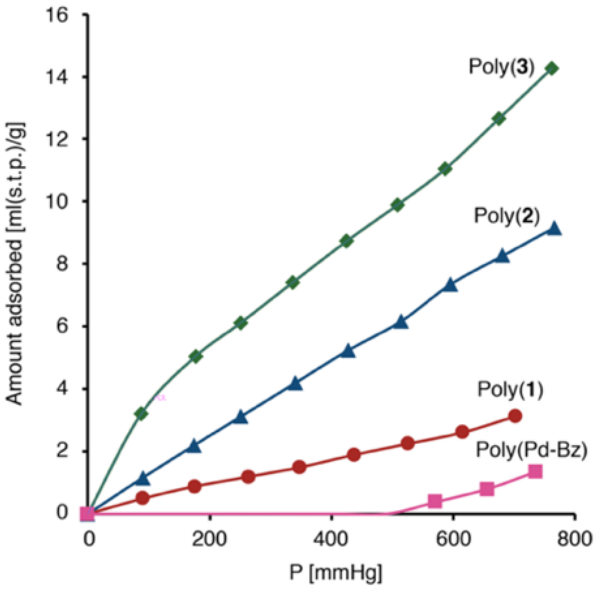

Fig. S50 CO_2 adsorption isotherms for poly(**1**)–poly(**3**) and poly(Pd-Bz) measured at 298 K.

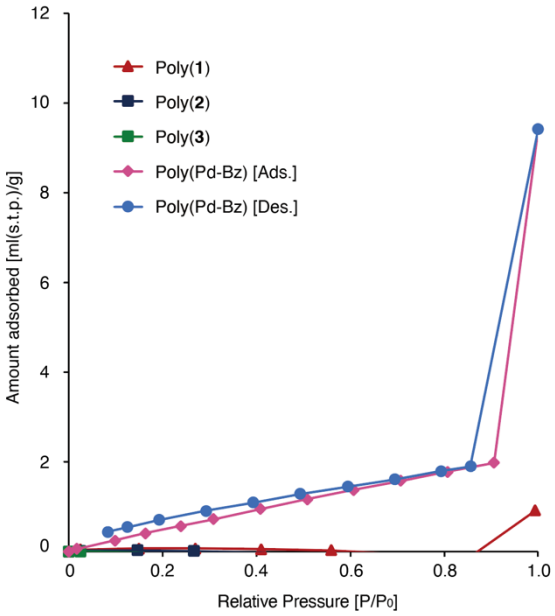

Fig. S51 N_2 adsorption isotherms for poly(**1**)–poly(**3**) and poly(Pd-Bz) measured at 77 K.

Table S2 Specific surface area, micropore and mesopore volumes of poly(**1**)–poly(**3**) and poly(Pd-Bz) determined using N_2

Compound	Specific surface area [a] [m^2/g]	Micropore volume [mL/g]	Mesopore volume [mL/g]
Poly(**1**)	0.3	0.000	– [b]
Poly(**2**)	0.0	0.000	– [b]
Poly(**3**)	0.0	0.000	– [b]
Poly(Pd-Bz)	0.0	0.000	0.007

[a] BET analysis. [b] Not determined.

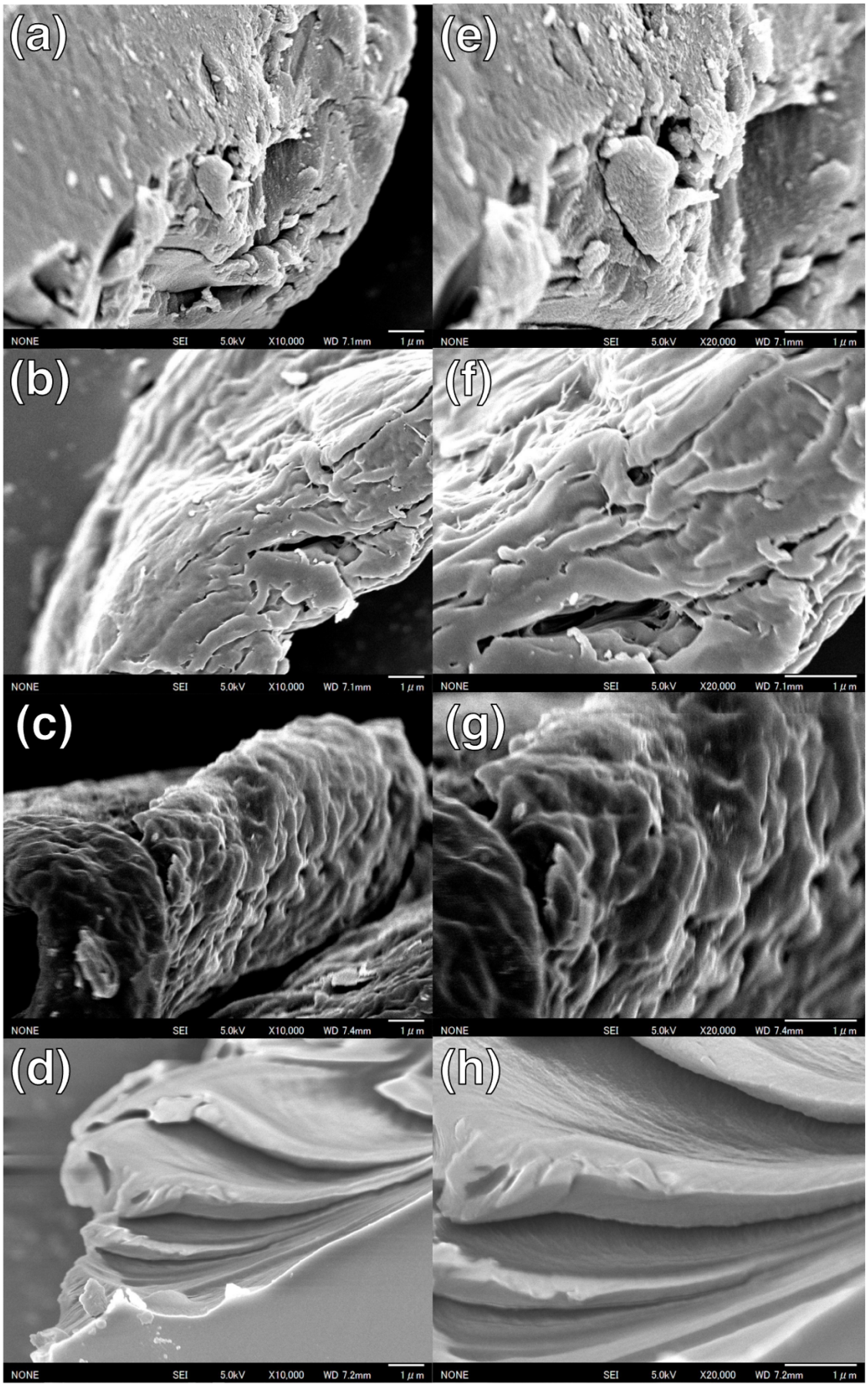

Fig. S52 FE-SEM images. (a), (e): poly(**1**), (b), (f): poly(**2**), (c), (g): poly(**3**), (d), (h): poly(Pd-Bz).

References

S1) O. V. Dolomanov, L. J. Bourhis, R. J. Gildea, J. A. K. Howard, H. Puschmann, *J. Appl. Cryst.*, 2009, **42**, 339–341.

S2) G. M. Sheldrick, *Acta Cryst.*, 2015, **A71**, 3–8.

S3) G. M. Sheldrick, *Acta Cryst.*, 2015, **C71**, 3–8.

S4) M. Goto, Y. Miyagi, M. Minami, F. Sanda, *J. Polym. Sci. Part A: Polym. Chem.*, 2018, **56**, 1884–1893.

S5) C. Mechtler, M. Zirngast, W. Gaderbauer, A. Wallner, J. Baumgartner, C. Marschner, *J. Org. Chem.*, 2006, **691**, 150–158.

S6) K. Yamashita, M. Tsuboi, M. S. Asano, K. Sugiura, *Synth. Commun.*, 2012, **42**, 170–175.

S7) T. Ozawa, *Polymer*, 1971, **12**, 150‒158.

S8) C. Jubsilp, S. Damrongsakkul, T. Takeichi, S. Rimdusit, *Thermochim. Acta*, 2006, **447**, 131–140.

S9) Y. Liu, Z. Yue, J. Gao, *Polymer*, 2010, **51**, 3722–3729.

S10) M. J. Frisch, G. W. Trucks, H. B. Schlegel, G. E. Scuseria, M. A. Robb, J. R. Cheeseman, G. Scalmani, V. Barone, G. A. Petersson, H. Nakatsuji, X. Li, M. Caricato, A. V. Marenich, J. Bloino, B. G. Janesko, R. Gomperts, B. Mennucci, H. P. Hratchian, J. V. Ortiz, A. F. Izmaylov, J. L. Sonnenberg, D. Williams-Young, F. Ding, F. Lipparini, F. Egidi, J. Goings, B. Peng, A. Petrone, T. Henderson, D. Ranasinghe, V. G. Zakrzewski, J. Gao, N. Rega, G. Zheng, W. Liang, M. Hada, M. Ehara, K. Toyota, R. Fukuda, J. Hasegawa, M. Ishida, T. Nakajima, Y. Honda, O. Kitao, H. Nakai, T. Vreven, K. Throssell, Jr. J. A. Montgomery, J. E. Peralta, F. Ogliaro, M. J. Bearpark, J. J. Heyd, E. N. Brothers, K. N. Kudin, V. N. Staroverov, T. A. Keith, R. Kobayashi, J. Normand, K. Raghavachari, A. P. Rendell, J. C. Burant, S. S. Iyengar, J. Tomasi, M. Cossi, J. M. Millam, M. Klene, C. Adamo, R. Cammi, J. W. Ochterski, R. L. Martin, K. Morokuma, O. Farkas, J. B. Foresman, D. J. Fox, Gaussian, Inc., Wallingford CT, 2019.

S11) E. R. Johnson, S. Keinan, P. Mori-Sańchez, J. Contreras-García, A. J. Cohen, W. Yang, *J. Am. Chem. Soc.*, 2010, **132**, 6498–6506.

S12) J. Contreras-García, E. R. Johnson, S. Keinan, R. Chaudret, J.-P. Piquemal, D. N. Beratan, W. Yang, *J. Chem. Theory Comput.*, 2011, **7**, 625–632.

S13) A. P. Thompson, H. M. Aktulga, R. Berger, D. S. Bolintineanu, W. M. Brown, P. S. Crozier, P. J. in 't Veld, A. Kohlmeyer, S. G. Moore, T. D. Nguyen, R. Shan, M. J. Stevens, J. Tranchida, C. Trott, S. J. Plimpton, *Comput. Phys. Commun*., 2022, **271**, 108171–108204.

S14) H. Chen, Y. Guo, Y. Du, X. Xu, C. Su, Z. Zeng, *Chem. Eng. J.*, 2021, **415**, 128824–128837.

S15) M. S. Jassim, G. Rochelle, D. Eimer, C. Ramshaw, *Ind. Eng. Chem. Res.*, 2007, **46**, 2823–2833.

S16) Q.-C. Ran, D.-X. Zhang, R.-Q. Zhu, Y. Gu, *Polymer*, 2012, **53**, 4119–4127.